Climate Dynamics
https://doi.org/10.1007/s00382-023-07095-w

ORIGINAL ARTICLE

Representing rainfall extremes over the Indo-Gangetic Plains using CORDEX-CORE simulations

Manas Pant[1,2] · Namendra Kumar Shahi[3] · Armelle Reca Remedio[4] · R. K. Mall[2] · Shailendra Rai[5] · R. Bhatla[1,2]

Received: 10 June 2023 / Accepted: 26 December 2023

Abstract
The Indo-Gangetic Plain (IGP), which is the site of India's Green Revolution, covers almost 15% of the country's landmass and is among the most extensively fertile lands across the world. The densely populated IGP region bears great importance for the socioeconomic facets of India and contributes to a major share of the GDP of the country. The present study demonstrates the regional-specific assessment of summer monsoon precipitation and associated extremes with dynamical and thermodynamical aspects over the IGP region using high-resolution regional climate models (RCMs) under the CORDEX-CORE framework. The analysis reveals that the eastern parts of the IGP receive low-to-moderate precipitation with a higher tail than the western parts, which is due to the direction of the monsoon low-level flow. The observed mean precipitation characteristics are well represented by the RCMs. Further, the research identifies extreme precipitation events over the IGP and conducts comprehensive analysis to understand their underlying mechanisms. It has been observed that extreme precipitation events are linked with the moisture transport associated with trough activity and instability, and RCMs are capable in representing the observed precipitation extremes and underlying mechanisms at localized scales. Overall, this study represents a significant step forward in understanding the evolution of spatio-temporal variability of precipitation over the IGP region, where agriculture is a major economic activity and millions of people depend on rainfed agriculture.

Keywords IGP · ISM · CORDEX-CORE · RCM · LLJ

1 Introduction

The Indo-Gangetic Plain (IGP) region is of great relevance to South Asia's food security as it produces 50% of foodgrains for more than 40% Indian population (Pal et al. 2009). The Indo Gangetic Plain (IGP) is drained by one of the world's largest river systems, as major rivers such as the Ganges, the Yamuna and the Brahmaputra flow through the region. Along with this the fertile alluvial plains so formed are frequently influenced by heavy rainfall and devastating floods and are now considered the worst flood-affected areas in the world (Kale 2003; New et al. 2012; Pant et al. 2023a, 2023b). Population growth and the development of industries have led to the emergence of numerous settlements in the floodplain areas. Consequently, flood and flash flood disasters have become ever-increasing natural disasters, causing the greatest economic damage of all types of natural disasters prevalent in the region. According to Kale (2003), the flood-induced variations were significant in parts of the IGP, resulting in changes in the dimensions, location and structure of major river channels and fertile lands. New et al. (2012) extensively studied the influence of climate change on agriculture in the IGP region. They projected that rainfed agriculture would become more viable for all crops due to expected precipitation increases. For irrigated farming, maize, wheat, and rice suitability remains unchanged, except in the warmest 2090s scenarios in the lower Indus valley. The agricultural activities in India and hence IGP region

✉ R. Bhatla
rbhatla@bhu.ac.in

1 Department of Geophysics, Institute of Science, Banaras Hindu University, Varanasi, India

2 DST-Mahamana Centre of Excellence in Climate Change Research, Institute of Environment and Sustainable Development, Banaras Hindu University, Varanasi, India

3 Institute of Environmental Geosciences (IGE), Grenoble Alpes University (UGA), Grenoble, France

4 Climate Service Center Germany (GERICS), Helmholtz-Zentrum Geesthacht, Hamburg, Germany

5 K. Banerjeec Centre of Atmospheric and Ocean Studies, University of Allahabad, Allahabad, India

Published online: 07 February 2024

are empathetically dependent on the Indian Summer Monsoon Rainfall (ISMR) which accounts for 80% of the annual rainfall of India. Thus, the ISMR which happens during June–September (JJAS), has a crucial impact on agricultural productivity and hence the gross domestic product (GDP) of the country (Gadgil and Kumar 2006). The seasonal rainfall over India undergoes variations in temporal as well as spatial aspects which leads the ISM systems to be complex, interesting, and important (Gadgil 2003). The dynamics of the Indian Summer Monsoon (ISM) circulation are influenced by factors spanning from global phenomena, such as El Niño Southern Oscillations (ENSO), Indian Ocean Dipole (IOD) to regional scales, including topography, land use, urbanization, and aerosols (Wang et al. 2009; Bajrang et al. 2023; Verma et al. 2023). Several authors have found an enhancement in the ISMR uncertainties in recent decades which leads to the amplification in the frequency and intensity of rainfall extremes such as flood and drought (Goswami 2005; Rajeevan et al. 2008; Shahi et al. 2018).

Among the most significant impacts of global warming are changes in the mean and extreme precipitation as the mean precipitation in a warming climate is anticipated to decline while the extreme rainfall events are on the rise (Groisman et al. 2005; IPCC 2013; Fadhel et al. 2018). The recent assessment report of the IPCC on climate change (IPCC 2013) emphasized the need of examining how different climate components behave during extreme rainfall events. The thermodynamic Clausius-Clapeyron relationship states that the concentration of atmospheric water vapour, which provides the water for precipitation, increases in proportion to the saturation concentrations at a rate of around 6–7% per degree rise in temperature (Allen and Ingram 2002; Trenberth et al. 2003). This is referred to as the thermodynamic response of rainfall extremes towards the warming climate (Pal et al. 2007). Along with thermodynamic aspects, the dynamical effects also bear great importance as well to the changes in atmospheric circulation at global and regional scales causing local changes in rainfall and associated extremes (Endo and Kitoh 2014; Freychet et al. 2015). Roxy et al., (2017) suggested that the increase in rainfall extremes over central India is the manifestation of enhanced variations in low-level westerlies over the Arabian Sea and the supply of moisture towards the Indian subcontinent. According to a study by Nikumbh et al., (2019), monsoon low-pressure systems may play a significant role in the increased occurrences of large-scale or widespread extreme rainfall events. The moist static energy (MSE) budget has been found to be a crucial factor in defining extended-scale impacts of climate on convective rainfall and climatology of rainfall over tropical regions (Bretherton 2006; Maloney 2009; Schneider et al. 2014; Sobel et al. 2014). According to a study by Field et al. (2012), the frequency of extreme rainfall events is increasing even though the intensity of mean rainfall is decreasing which may cause significant impacts on livelihood. From the Indian perspective, the rainfall extremes are on the rise while the moderate rainfall episodes are decreasing (Goswami et al. 2006; Roxy et al. 2017). In the recent past, India has faced several rainfall extremes, for example, extreme rainfall over Mumbai in 2005 (Pant et al. 2022), the 2013 Uttarakhand floods (Joseph et al. 2015) and the Kerala floods in 2018 (Mishra and Shah 2018) etc. As per the report of the International Disaster Database, in India, around 268 floods and flash floods, events affected 825 million people with 69,000 casualties and 17 million became homeless during 1950–2015 (http://www.emdat.be). Thus, the analysis of rainfall extremes and associated governing physical processes for better estimation of occurrence is a challenging matter of concern for the scientific community.

Some earlier studies have found the reliability of the global climate model (GCM) in predicting the weather and climate under warming scenarios across the world (Xu et al. 2018; Rogelj et al. 2019). The models under Coupled Model Intercomparison Project phase 5 (CMIP5) framework have projections of enhanced ISMR and an increase in intensity and frequency of extreme rainfall over Indian regions under warming climate scenarios (Ramesh and Goshwami 2014; Sharmila et al. 2015; Maity et al. 2016; Vittal et al. 2016). In other studies, using CMIP5 models, Singh and Goyal, (2016) proposed intensification in the rainfall extremes over the eastern Himalaya region while Woo et al., (2019) found a projected increase in the ISMR over northwest and northeast India in the future. The successor of the CMIP5 framework i.e., CMIP6 can also represent improved climatic patterns and has also shown enhanced projections of the ISMR and associated extremes over Indian regions (Gusain et al. 2020; Shahi et al. 2022). However, the GCMs broadly capture large-scale circulations reasonably well but their skills are limited in representing realistic patterns at a regional scale due to their coarser resolution (Sinha et al. 2013; Sharmila et al. 2013; Ashfaq et al. 2021; Shahi et al. 2021, 2022). Therefore, to overcome the difficulties of GCMs, the concept of dynamical downscaling using a regional climate model (RCM) was introduced which provides more resolved (being high-resolution) climatic patterns at lower computing costs (Giorgi et al. 2009; Giorgi and Gutowski Jr 2015; Kang et al. 2015). Also, if the resolution is increased, the RCM simulations lead to more accuracy due to improvised representation of topography, land-surface process, coastlines and other dynamical processes at localized scale as compared with GCMs (Kumar et al. 2013). In that view, during the recent decade, numerous studies have been conducted to access the ISM circulation pattern and ISMR variability with RCMs over India and its subregions (Pal et al. 2007; Giorgi et al. 2012; Bhatla et al. 2016, 2018, 2019a; Maharana and Dimri 2014, 2016; Ghosh et al. 2019, 2022, 2023; Verma et al. 2021, 2022b).

The CORDEX framework was developed under World Climate Research Programme (WCRP) to provide high-resolution climatic information over multiple domains across the globe (Giorgi et al. 2009). In the first phase of CORDEX, various studies have been carried out over the South-Asia domain (one of the 14 proposed CORDEX domain; SA-CORDEX hereafter) to study the characteristics of the ISM (Singh et al. 2017; Choudhary and Dimri 2019). Several studies have observed the deceptive biases in monsoon precipitation over the Indian landmass using the first phase of the SA-CORDEX simulations, which may be due to the horizontal resolution (~ 50 km) of simulations (Rana et al. 2020; Sanjay et al. 2020). To address the uncertainties with the CORDEX simulations, the WCRP community developed the finer resolution (~ 25 km) Coordinated Output for Regional Evaluations (CORDEX-CORE) programme for its existing CORDEX domains (Giorgi 2021). Previously, several authors have evaluated the performance of different RCMs participating in the CORDEX-CORE framework in analysing the present and future aspects of ISM (Varikoden et al. 2018; Choudhary and Dimri 2018, 2019; Maharana et al. 2019; Shahi et al. 2021; Shahi and Rai 2023). Maharana et al. (2019) used RCMs to show that the earlier onset of ISM is possible due to an increase in an anthropogenic influence on air temperature under 1.5 °C and 2 °C warming levels. The CORDEX-CORE simulations can represent the mean and extreme ISM characteristics and region scale and are more reliable for regional assessment of climate change over the region of interest (Pant et al. 2023a). In a study by Verma et al., (2022b) with the high-resolution RCMs (RegCM4.7, COSMO & REMO2015) simulation demarcated the localized hotspots susceptible to drought and flood along with decreasing trends in ISMR over the northeast and north central Indian regions. Similarly, another study of Maharana et al. (2021) evaluates the capability of earlier mentioned RCMs in simulating ISMR patterns and found RCM COSMO performing robustly over Indian regions in simulating the mean ISMR and associated extremes. A regional study over the Himalayan region has been conducted to showcase the rainfall variability and future projections show an increase in rainfall over the eastern Himalayan region (Choudhary and Dimri 2018). However, one of the socioeconomically vulnerable regions, the IGP (as discussed earlier) is still unnoticed as far as the ISMR patterns, rainfall extremes and governing physical processes are concerned which is the scope and motive of the present study. Though, few researchers have attempted to access the ISM features and variability over IGP regions (Singh and Sonatakke 2002; Yaduvanshi and Ranade 2017; Bhatla et al. 2015, 2019b, 2020; Singh and Bhatla 2020). Another study of Bhatla et al., (2019b) exclusively focussed on different category extreme rainfall events and found an increasing trend in moderately heavy rainfall episodes whereas a substantial decline in very heavy rainfall events. However, some modelling-based approaches such as CMIP5 proposed a significant increase in the mean and extreme temperatures over IGP (Chauhan et al. 2014; Sanjay et al. 2017). Using a multimodal ensemble mean, Chaturvedi et al. 2012 proposed 10% and 20% of enhancement in rainfall during the 2030s and 2080s respectively. Pant et al., (2023a, b) exclusively focussed on the ISM rainfall and associated extremes over IGP region and a projected enhancement in the intensity and frequency of heavy rainfall which is may be due to the strengthening of tropospheric temperature gradient and availability of enormous amount of moisture in the atmosphere. The aim of the present study is to analyse the comprehensive rainfall characteristics and associated extremes along with the dynamical and thermodynamical aspects over the IGP region which bears great economic importance. For that purpose, the high-resolution CORDEX-CORE RCM simulations (Teichmann et al. 2021) have been considered for the period of 1981–2005.

2 Model description and methodology

The daily gridded observation data at 25 km horizontal resolution provided by India Meteorological Department (IMD) for the period 1981–2005 has been considered for model evaluation (Pai et al. 2014). The model domain (SA-CORDEX) and topography (m) with highlighted study region have been illustrated in Fig. 1. The high-resolution dynamically downscaled CORDEX-CORE simulation (~ 25 km) of three RCMs namely ICTP's RegCM4.7, ETH Zürich-Switzerland's COSMO-crCLIM-v1-1 and GERICS-Germany's REMO2015 have been considered in this study (Table 1). All the CORDEX-CORE simulations are driven by common initial and boundary conditions (ICBCs) derived from the Norwegian Earth System Model (NOR-ESM1-M; Bentsen et al. 2013) during the period of 1979–2005. Pant et al., (2023a) found RegCM4.7 forced with NOR-ESM1-M model performs better over IGP region in simulating ISMR patterns. The state-of-the-art RegCM4.7 model developed at Abdus Salam International Centre for Theoretical Physics (ICTP), Italy has been considered with its hydrostatic core option for the simulation (Giorgi et al. 2012). The Consortium for Small-scale Modelling (COSMO-CLM; Baldauf et al. 2011) model developed by the Climate Limited-area Modelling Community (CLM-Community) is a non-hydrostatic model and its latest version COSMO-crCLIM-v1-1 has been used for simulation (Asharaf and Ahrens 2015; Sørland et al. 2021). The latest version of REMO (REMO2015) with its hydrostatic dynamical solver has been considered for the simulation by its host institute i.e., GERICS, Hamburg, Germany (Jacob et al. 2012; Remedio et al. 2019). All the RCM simulations have been considered for the period

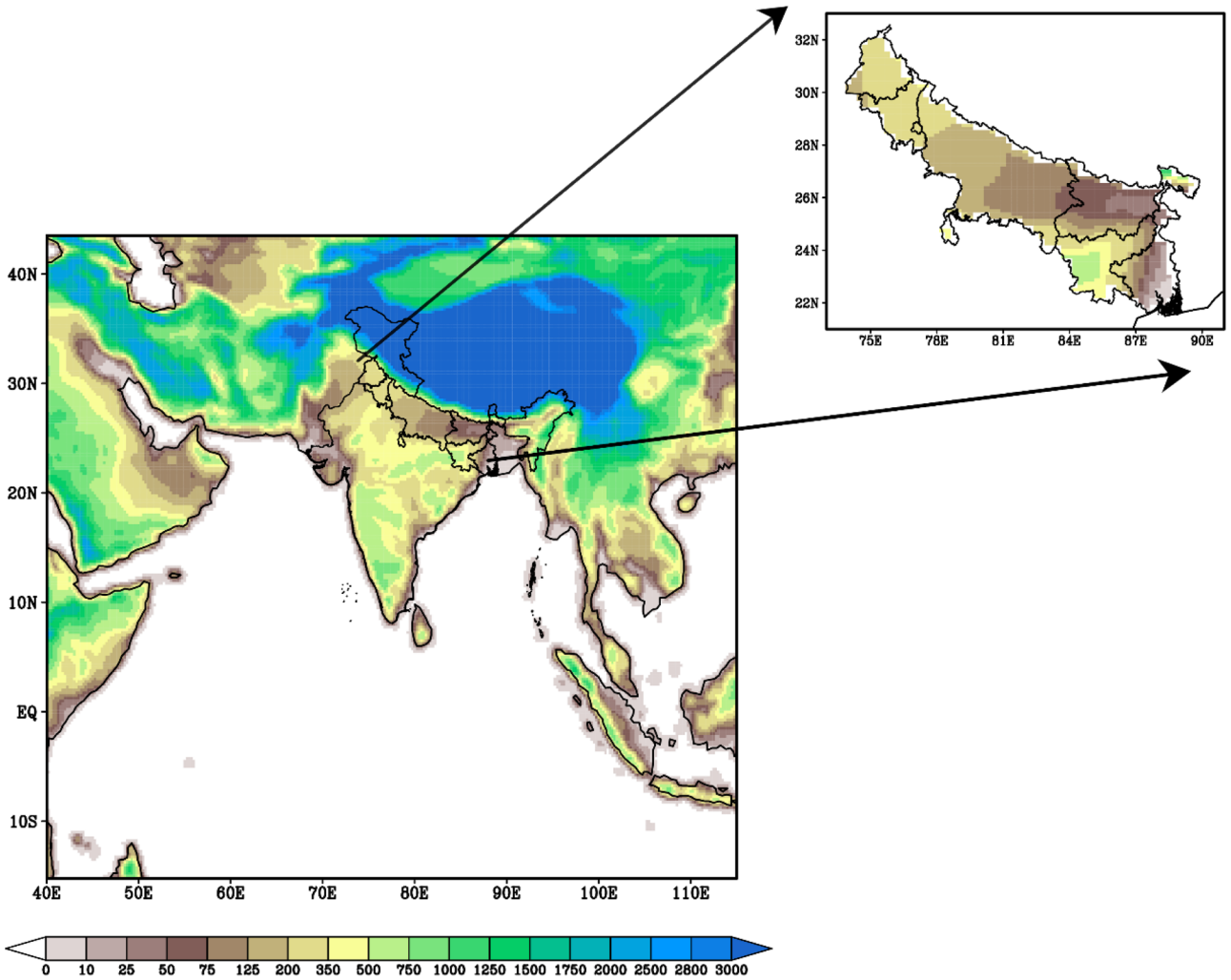

Fig. 1 Topography (m) of South-Asia CORDEX domain considered as model domain. The small rectangular box shows the Indo Gangetic Plain (IGP) study region highlighted on the right side of the figure

1981–2005 with the first two years (i.e., 1979–1980) of the simulations considered as the spin-up time for the model. In addition to precipitation, several other variables such as temperature (T), zonal (u) and meridional (v) winds, specific humidity (q), geopotential height (Zg), and water vapour path (prw) from the RCM simulations and ERA5 (Hersbach et al. 2020) reanalysis have been used to study relevant physical processes. All the data sets have been detrended before the analysis.

For the model evaluation purpose, the widely used Taylor diagram and probability distribution function (PDF) have been considered. The Taylor diagram is an extensively used statistical technique for evaluating model performance in reproducing the climate features over a region of interest (Taylor 2001). It provides a comprehensive assessment based on standard statistics such as correlation coefficient (CC), standard deviation (SD), and root mean square error (RMSE). Further, the PDF is used to demonstrate the overall intensity-frequency distribution of observed and RCM-simulated precipitation over the IGP region (Shahi et al. 2022).

To showcase the physical processes, various dynamical and thermodynamic variables have been calculated. In the present study, the moisture transport (MT) and horizontal moisture flux convergence (HMFC) at 850 hPa have been analysed to investigate the atmospheric water transport over IGP.

The MT (at 850 hPa) is calculated using the given equation

$$MT = q_{850} U_{850}(u, v) \tag{1}$$

And the HMFC calculation at 850 hPa has been performed as follows:

$$HMFC = -\left(\frac{\partial (q * u)_{850}}{\partial x} + \frac{\partial (q * v)_{850}}{\partial y} \right) \tag{2}$$

Similarly, to account the land thermal forcing and moist processes and its effects on mean and extreme rainfall during the ISM season the moist static energy (MSE) has been computed at 850 hPa. Also, the MSE differences between levels 500 hPa and 925 hPa have been considered for the sake of atmospheric instabilities during and before the extreme rainfall events. The MSE calculations has been performed as follows (Sooraj et al. 2020),

$$MSE = C_pT + Lq + gz \quad (3)$$

where Cp ~ 1.005 kJ/kg-K (for air) is the specific heat capacity at constant pressure, T is the air temperature at the concerned level, L being the latent heat of vaporisation at 0 °C, q is the specific humidity, g is the acceleration due to gravity and z being the geopotential height.

3 Identification of the rainfall extremes

In the next evaluation step, we focus on the representation of heavy/extreme precipitation. Basically, we extracted the days with extreme precipitation from the time period of our study. Extreme precipitation days are defined as days in which at least 20% of the grid points from the total grid points of the study domain meet the 95th percentile threshold values. The 95th percentile of daily mean precipitation has been calculated for the time period of our study.

4 Results and analysis

4.1 The Spatio-temporal distribution of mean ISMR

The spatial distribution of the observed and model-simulated summer mean precipitation and associated biases over IGP during the period 1981–2005 has been illustrated in Fig. 2. Climatologically, the western parts of IGP receive less precipitation than the eastern parts and this is due to the monsoon features i.e., low-level moisture-laden wind flow directions. Observations (IMD) reported ~ 10–12 mm/day over the lower or eastern IGP regions whereas moderate mean precipitation in the range of ~ 3–8 mm/day occurs over the central IGP region which further decreases towards upper IGP (~ 2–4 mm/day) (Fig. 2a). The ERA5 reanalysis depicts the similar distribution of precipitation pattern over the IGP region with a smaller wet bias (1–2 mm/day) over the entire IGP region which agrees with the study of Rani et al., (2021) (Fig. 2b and h). As far as modelling aspects are concerned, the Nor-ESM GCM shows the unresolved mean ISMR pattern as compared to the observation, which may be due to the horizontal resolution of the GCM (Fig. 2c). Noticeable wet (4 mm/day or more) and dry (5 mm/day or more) biases over northern and southern IGP regions can be seen, respectively (Fig. 2i). As can be seen from Fig. 2d-g, all the considered RCMs have systematically reduced (1–3 mm/day or less) the parent GCM biases up to a great extent. The RegCM4 satisfactorily reproduces the observed mean precipitation pattern over IGP region and is able to reduce the larger wet biases (~ 1 mm/day) over northern IGP regions as compared with its forcing (Fig. 2d and j), however, considerable dry biases (3 mm/day or more) are present over southern and lower IGP regions. Earlier, some researchers have found large underestimations of summer mean precipitation in RegCM simulations over central India and Gangetic plain regions (Choudhary et al. 2019; Bhatla et al. 2019a, b), however, the recent version (used here) with CORDEX-CORE simulations have robustly improved it (Shahi et al. 2021; Verma et al. 2022a, b). Maharana et al., (2019) accused the use of CLM4.5 in RegCM simulations for the overestimations in ISM rainfall. Another member COSMO performs robustly and reduces the inherent lateral boundary conditions (LBCs)-associated errors and shows a more realistic pattern of rainfall over the entire IGP region (Fig. 2e and k). However, slight dry biases (− 1 to − 2 mm/day) have been found over the central IGP region in COSMO simulations. Similarly, REMO satisfactorily reproduces the mean ISMR over the considered region (Fig. 2f). However, it has shown slight underestimation or dry biases over the entire IGP region as compared with the observations (Fig. 2l). At last, the RCM-MME shows realistic patterns over the entire IGP except for lower IGP where it has shown smaller dry biases (Fig. 2g and m). The RCM have demonstrated a consistent tendency to underestimate seasonal average precipitation across most of the study area. In contrast, ERA5 exhibits a diverse bias pattern, primarily characterized by a slight overestimation in most regions. The overall discussion suggests COSMO performed best among all the considered models and the use of RCM-MME further represents the mean ISMR pattern with reduced wet/dry biases (making it closer to the observation) during the historical period.

The ability of different RCMs in reproducing the observed spatial characteristics of precipitation over the IGP has been investigated using the Taylor diagram (Taylor 2001) which combines the spatial correlation coefficient (CC), Standard Deviation (SD), and the root mean square error (RMSE). It has been observed that all the RCMs and its MME have shown correlation values above 0.8 (Fig. 3). The parent GCM Nor_ESM has shown lesser correlation (~ 0.6) as compared to downscaled RCMs, which resembles the capability of RCMs in reproducing regional features to a greater extent. Further, comparative analysis among the RCMs suggests COSMO and the RCM-MME performed best among all the considered experiments with the highest CC (~ 0.93) with the least RMSE (~ 0.4 or less) in simulating mean precipitation pattern over IGP during 1981–2005. Furthermore, the

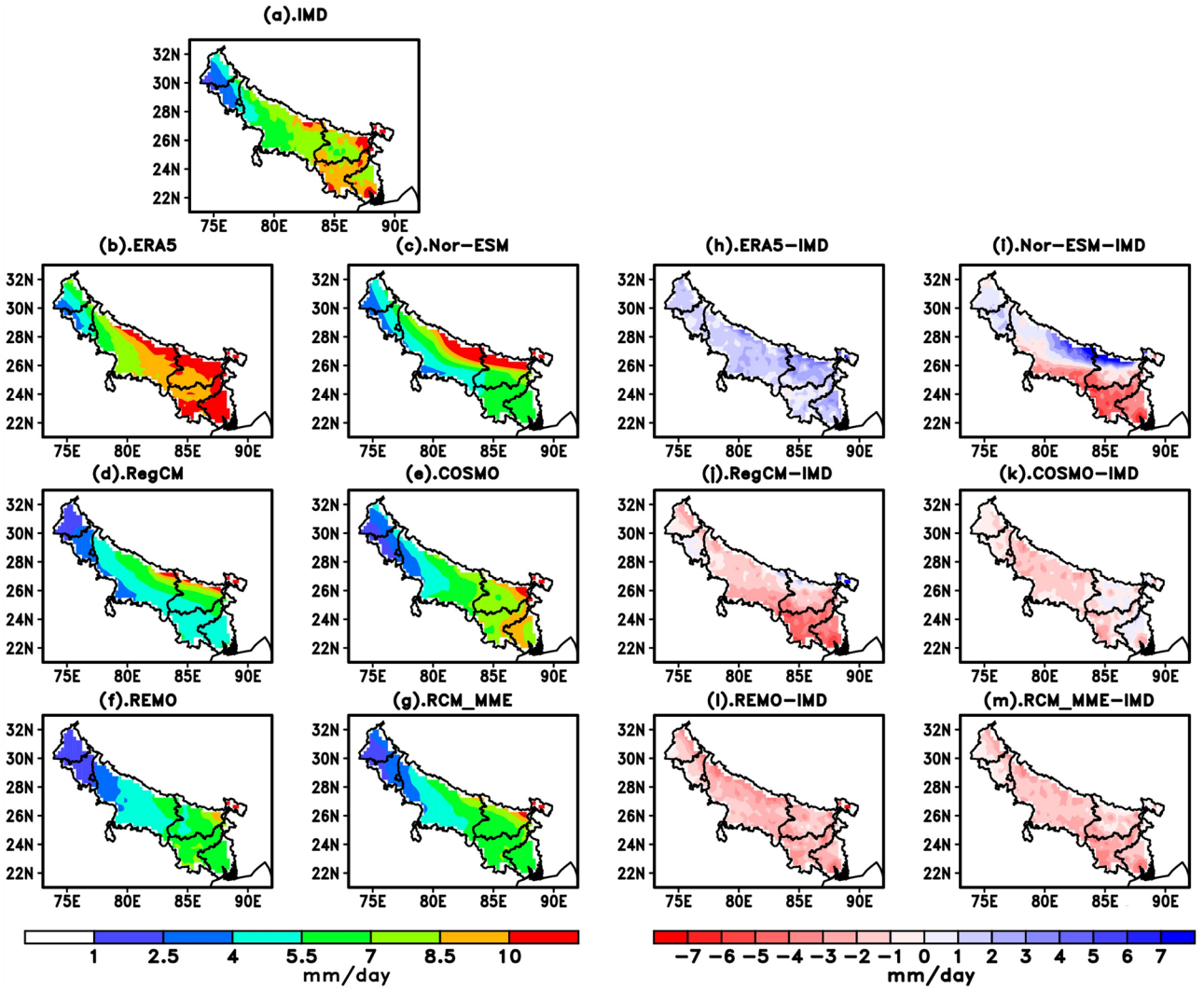

Fig. 2 Spatio-temporal distribution of (**a**). Observed (IMD) (**b**). Reanalyses (ERA5), (**c**). GCM simulated (Nor-ESM) and (**d**–**g**). RCM simulated (RegCM, COSMO, REMO and RCM-MME) mean ISM rainfall and respective biases (**h**–**m**) with observations over IGP region during 1981–2005

REMO followed by RegCM has shown reasonable performance with CC of 0.85 and 0.8, respectively.

4.2 Dynamical and Thermodynamical aspects of the ISMR

As mentioned earlier, this study focuses on the evaluation of rainfall extremes and associated thermodynamic aspects. Therefore, here a comprehensive analysis of variables temperature (T), wind with MT, geopotential height (Zg850) and moist static energy (MSE) during the ISM season has been discussed. The distribution of temperature at 850 hPa has been represented in (Fig. 4). The ERA5 reanalysis shows maximum temperature (24–28 °C) over the heat-low (one of the semi-permanent features of the ISM circulation) and Indo-Pak arid region (Bollasina and Nigam 2011) which decreases towards the north (20–22 °C) and southeastern Indian regions (18–20 °C) (Fig. 4ia). The central India region reported up to 22 °C while the peninsular region has shown temperatures below 20 °C during the period. Further, the mean temperature distribution over the IGP shows maximum value over the upper region which subsequently decreases as moving towards the central and lower IGP. The RegCM satisfactorily reproduces temperature patterns over the entire region, however, it shows overestimations (22–24 °C) over central India and IGP regions which might be due to the inherent uncertainty within the forcing Nor_ESM (Fig. 4ic). Also, a massive overestimation over the Himalayan and its northward can be noticed in RegCM simulations. The REMO shows a more realistic

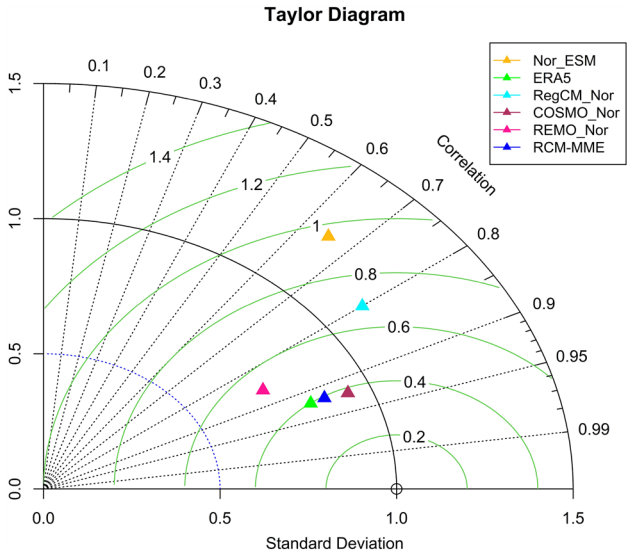

Fig. 3 Taylor's diagram for GCM and RCM simulated mean ISM pattern over IGP during 1981–2005

distribution pattern of temperature than RegCM over the entire considered region (Fig. 4id). However, it also exhibits some overestimations over north-western India and beyond the Himalayan regions during the period. The model COSMO surprisingly reproduces the temperature pattern up to a great extent over the entire Indian Subcontinent and the region of interest i.e., the IGP (Fig. 4ie). Also, the overestimated temperature pattern beyond the Himalaya and the Tibetan plateau region is absent in the COSMO simulation as compared to the other RCM simulations. Further, the RCM-MME has well captured the temperature distribution over considered regions during the historical period (Fig. 4if). The wind and transport of moisture at 850 hPa have been depicted in Fig. 4ii. The wind at 850 hPa also known as low-level jet or the Findlater jet of the ISM circulation plays a vital role in transporting moisture towards the Indian landmass from oceanic regions (Goswami 2005). The ERA5 reanalysis depict intense low-level jet (more than 12 m/s) over the Somalia region which

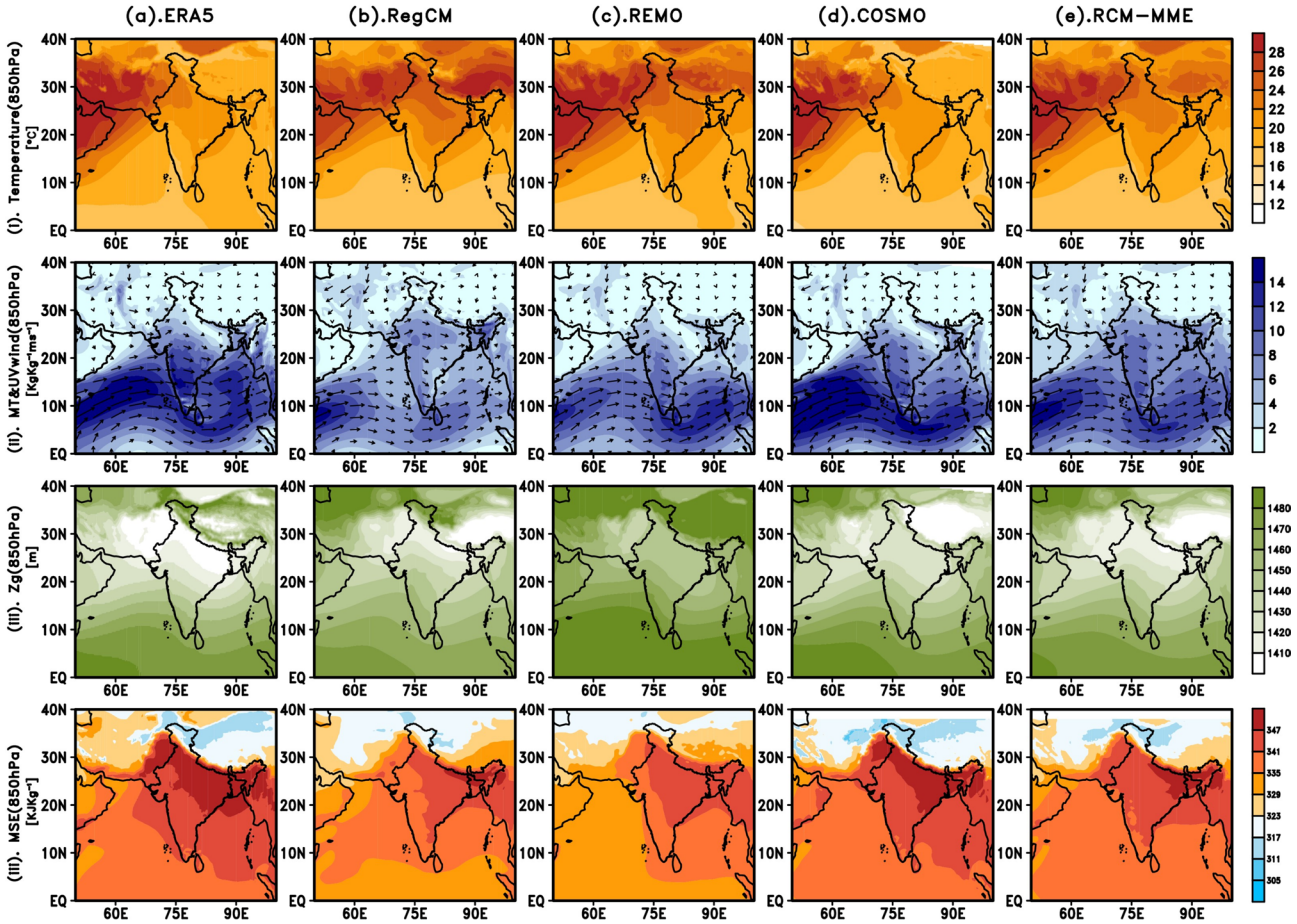

Fig. 4 Spatial distribution of reanalyses (ERA5) and RCM simulated mean Temperature, MT & Wind, Zg850 and MSE at 850 hPa for ISM season during 1981–2005

further slightly reduces towards the land regions although it is sufficient to supply the enormous moisture over western India (Fig. 4iia). All the considered models have captured the cross-equatorial flow and strong low-level jet reasonably well (Fig. 4iie–f). The wind strength is slightly underestimated in RegCM and REMO simulations as compared to the ERA5. Further, the transport of moisture (MT) with the wind towards the land regions is clearly visible in all the RCMs as well as the RCM-MME. The COSMO model has shown a more realistic pattern among the considered models in the context of wind speed and its direction while RegCM has underestimated the presence of moisture content over the western coast, the Bay of Bengal (BoB) and hence the Indian land. The lesser moisture content in RegCM simulations is due to the weakened low-level jet which consequently might be a region of dry biases over western and central Indian regions in RegCM simulations. The geopotential height accounts for the actual height of the pressure surface above sea level and is useful to locate ridges and troughs over a region (Thompson et al. 1998). Therefore, the presence of monsoon troughs or low-pressure regions, the distribution of geopotential height at 850 hPa (Zg850) has been shown in (Fig. 4iii). The minimum Zg850 values can be clearly observed in the ERA5 distribution from the northern BoB to western India which explains the flow of moisture transport in the region and hence the summer monsoon precipitation. (Fig. 4iiia). As far as modelling aspects are concerned all the models have reproduced the presence of a low-pressure belt as we observed from ERA5 (Fig. 4iiic-e). However, inter-model differences can be clearly observed, but the RCM-MME robustly determines more realistic patterns (Fig. 4iiif). Similarly, the distribution of MSE at 850 hPa has been illustrated in Fig. 4iva-e. The ERA5 reanalysis reported the highest MSE build-up (347 kJ/Kg and more) extending from northern BoB to the Indo-Pak arid regions during the summer monsoon season. This highest MSE build-up also covers the north-central and entire IGP region including the Himalayan foothills. During the daytime, the moisture content at lower levels gets limited due to the increased atmospheric stability (caused by absorbing aerosols) over polluted urbanized regions such as IGP. The accumulated MSE at lower levels gets transferred towards the foothills during the night and results in extremely heavy rainfall episodes due to the orographic lifting (Fan et al. 2015; Choudhury et al. 2020). The maximum convective instability during ISM season exists over the monsoon trough and adjoining regions and higher MSE manifests the enhanced intrusion of moisture increasing the lower-level convergence which causes extreme rainfall to occur over the region of interest (Saha and Sateesh 2022). The oceanic regions have shown lesser MSE values as compared to the land regions ranging from 323 to 241 kJ/Kg. As far as the modelling aspects are concerned the RegCM has satisfactorily reproduced the MSE over the entire domain with slight underestimations in comparison with the ERA5. However, RegCM robustly captures the higher MSE build-up over foothill regions. Another model, COSMO, shows a more realistic pattern over MSE at 850 hPa over the considered region including IGP. The performance of COSMO is also up to the mark over oceanic regions. Further, the RCM-MME shows a similar pattern as that of COSMO but with a slight underestimation over Indo-Pak arid region and central IGP regions. To investigate the physical processes more precisely for the IGP region, the temporal distribution of earlier discussed parameters (daily mean during JJAS; 122 days) by area averaging over IGP has been illustrated in Fig. 5. The ERA5 distribution of daily mean temperature shows maximum temperature (27 °C) during the early phase of the ISM days (i.e., during June) which gradually decreases (22 °C) up to the middle of the ISM (end of July) (Fig. 5a). Afterwards, the temperature almost stabilizes (slight fluctuations) for the rest of the season. The RegCM simulation shows massive overestimation (26–28 °C) in daily temperature from mid-June to mid-September and a steep decline at the end of the ISM season which is also visible in mean seasonal temperature variations over the IGP (Fig. 4ic). The COSMO shows a similar pattern as that of ERA5 reanalysis but with an underestimation throughout the season. However, the model REMO and MME reproduce a more realistic pattern with greater accuracy as compared with ERA5. The temporal variation of the MT at 850 hPa in the ERA5 reanalysis suggests a gradual increase from the beginning of June which reaches its maximum during July–August months and decreases substantially at the end of the ISM season (Fig. 5b). The modelling aspects show the RCM-MME being the best fit with the ground truth ERA5 reanalysis rather than individual model simulation throughout the season. All the considered models have shown overestimation in its MT during the peak ISM season (July–August) over the IGP region. Similarly, the temporal variation of Zg at 850 hPa shows a gradual decline from the beginning of the season up to the peak monsoon season then increases afterwards in ERA5 distribution which suggests the genesis and presence of monsoon trough over the IGP during the ISM season. The ERA5 distribution of Zg850 shows a fluctuating pattern between 1350 and 1450 m during the historical period (Fig. 5c). As far as modelling aspects are concerned, all the considered models and MME have reproduced the Zg850 pattern reasonably well throughout the period. However, fluctuations in Zg850 values are very rare in RCM simulations. Further, the reanalysis MSE distribution shows an increasing pattern (335 kJ/Kg) from the beginning of the season which reaches its maximum (~ 360 kJ/Kg) during the mid-ISM

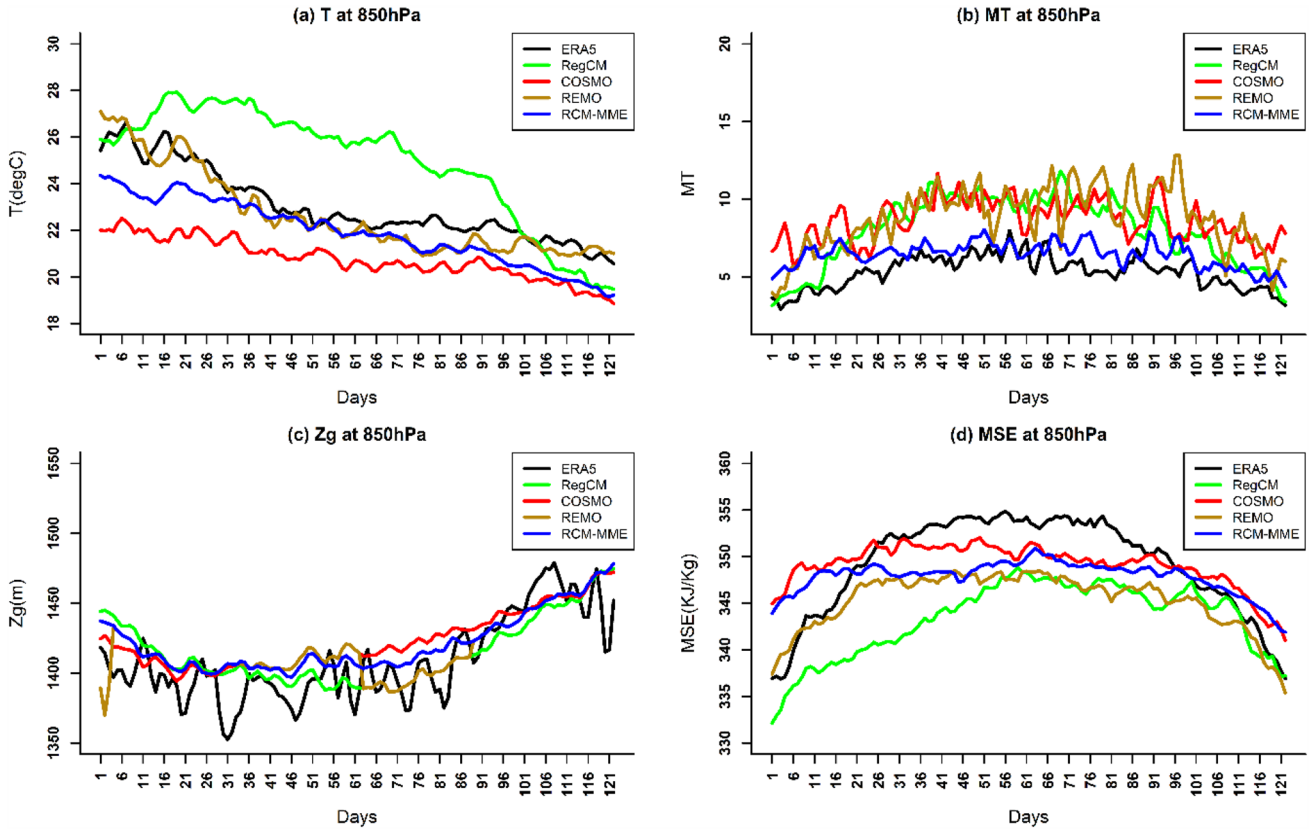

Fig. 5 Temporal distribution of reanalyses (ERA5) and RCM simulated mean (area averaged over IGP region) Temperature (T), MT & Wind, Zg850 and MSE at 850 hPa for ISM season during 1981–2005

season and decreases towards the end of the season (Fig. 5d). Among all the considered RCMs and MME have satisfactorily reproduced the MSE pattern throughout the ISM season with slight fluctuations as compared with ERA5 reanalysis distribution. However, the RegCM have shown an underestimated distribution of MSE which might be the cause behind uncertainties with rainfall patterns in RegCM simulations.

Table 1 Detailed RCM description

	REGCM4	COSMO	REMO2015
Institute	ICTP	CLMcom-ETH	GERICS
Version	RegCM4.7	COSMO-crCLIM-v1-1_v1	REMO2015_v1
Dynamics	Hydrostatic		
Domain	South Asia CORDEX domain (22° S–50° N; 10° E–130° E)	South Asia CORDEX domain (22° S–50° N; 10° E–130° E)	South Asia CORDEX domain (22° S–50° N; 10° E–130° E)
Resolution	25 km	0.22°	0.22°
Vertical levels	23	57	27
PBL	Holtslag PBL (Holtslag et al. 1990)	–	Monin–Obukhov similarity theory (Louis 1979)
ICBC	NCC_Nor_ESM-1-M	NCC_Nor_ESM-1-M	NCC_Nor_ESM-1-M
CPS	Emanuel over Land & Tiedtke over Ocean	Tiedtke (1989)	Tiedtke (1989)
Microphysics	SUBEX (Pal et al. 2000)	–	Lohmann and Roeckner (1996)
Period	1981–2005	1981–2005	1981–2005

4.3 Analysis of rainfall extremes over IGP and associated physical processes

4.3.1 Spatio-temporal distribution of extreme rainfall patterns:

After building our analysis on the mean ISMR characteristics over the IGP along with its dynamical and thermodynamical aspects, the rainfall pattern for monsoon extremes has been discussed in the present section. The 95th percentile of the daily rainfall (R95p) during ISMR has been considered to identify extreme rainfall events i.e., the days when above 95th percentile of rainfall amount has occurred will be termed as an event (R95p days hereafter) during the historical period. The distribution of R95p has been shown in Fig. 6. Observations have reported a maximum 70-90 mm or more R95p over Himalayan foothills and some isolated northern regions over lower and central IGP (Fig. 6a). Most of the IGP region have shown 50-80 mm of threshold while upper IGP (the north-western region) have reported 50 mm or less rainfall thresholds during the period. The reanalysis ERA5 also depicts similar distribution as that of IMD but with lesser rainfall amounts over respective regions (Fig. 6b). As far as the RCM simulations are concerned the model RegCM has reproduced the pattern satisfactorily but it slightly underestimates the R95p thresholds over lower IGP and southern parts of central IGP (Fig. 6c). Another member COSMO (Fig. 6c) performs reasonably well over the entire IGP region but it has shown slight underestimations over northern regions of central IGP (specially the foothills of Himalaya). The uncertainty in extreme values over northern regions may be due to the poor representation of topography and various physical processes in RCM. The REMO model reproduces R95p thresholds to a great extent over almost the entire IGP as compared with observations (Fig. 6e). However, it has overestimated the R95p over some isolated southern lower IGP regions. Similarly, the RCM-MME is also in good agreement with the observations (Fig. 6f). Now, based on this discussion, the R95p days have been chosen across the various datasets. The composites of those identified days have been illustrated in Fig. 7. The observed pattern depicts a maximum of 35-47 mm/day or more rainfall over lower and north-central IGP regions while the rest of the IGP regions have reported 11-35 mm/day of scattered rainfall pattern (Fig. 7a). The Himalayan foothills fall under the upper tail of the distribution which may be due to the enhanced aerosol concentrations (Choudhury et al. 2020). The composite pattern with reanalysis ERA5 also depicted a similar pattern but with lesser intensities over almost the entire IGP region during the R95p days (Fig. 7b). The RCM simulations have also reproduced the observed pattern up to great accuracy (Fig. 7c–e). The RegCM (Fig. 7c) satisfactorily simulates the composite over the region but it shows slight to higher overestimations over southern regions of central IGP while underestimations over Himalayan foothills. Further, the COSMO simulation closely resembles the realistic patterns of R95p days in terms of both intensity as well as a distribution over the entire IGP region (Fig. 7d). Another member REMO also reproduces the composite pattern reasonably well over the entire IGP except central IGP where it has shown moderate to higher overestimations during the period (Fig. 7e). Similarly, the RCM-MME represents the composite pattern with great accuracy over the IGP region during the R95p days (Fig. 7f). Pai et al. (2014) proposed that IMD gridded datasets may not accurately reflect areas with limited rain gauge data, especially in the western and central Indo-Gangetic plain. In such regions, the interpolation method used for generating gridded data has limitations (Prakash et al. 2015). Consequently, any estimates of extremes by the model in these regions might not necessarily be wrong/incorrect. To investigate the capability of RCMs in simulating R95p days or rainfall extremes over IGP, the Taylor diagram for spatial pattern of R95p days has been illustrated in Fig. 8 (as similar to Fig. 3). The ERA5 reanalysis shows CC ~ 0.7 w.r.t., observations while the RCMs COSMO and RegCM have shown CC > 0.7. However, REMO shows lesser CC ~ 0.6 during the period. Further, the RCM-MME also shows higher CC (> 0.7) which suggests the potential ability of RCMs in capturing extreme rainfall events at a regional scale. A slight underestimation in the case of extreme precipitation has been observed in ERA5, although the spatial pattern simulated by ERA5 is more comparable to observations than the RCMs. The monthly distribution (%) of above R95p days has been shown in Table 2. As per the IMD distribution, September month has shown the highest event frequency (40%) compared to other months. The table also verifies the presence of events in June in observed as well as simulated data sets. The ERA5 distribution have shown more events than IMD, the distribution across the months remains consistent with the observations. The RCM simulated event count matches the observations, though differences in monthly contributions are evident.

4.3.2 Dynamical and Thermodynamical aspects of rainfall extremes over IGP

To understand the thermal and dynamical aspects or to resolve the physical processes associated with rainfall extremes, the composite distribution patterns of temperature (T), wind with MT and HMFC at 850 hPa has been illustrated in (Fig. 9). The ERA5 reanalysis temperature shows maximum values over the Indo-Pak arid (24–28 °C) and western Indian (20–22 °C) regions while lowest temperature over central India (20–22 °C) and IGP (18–20 °C) region have been reported (Fig. 9ia). All the RCMs (including

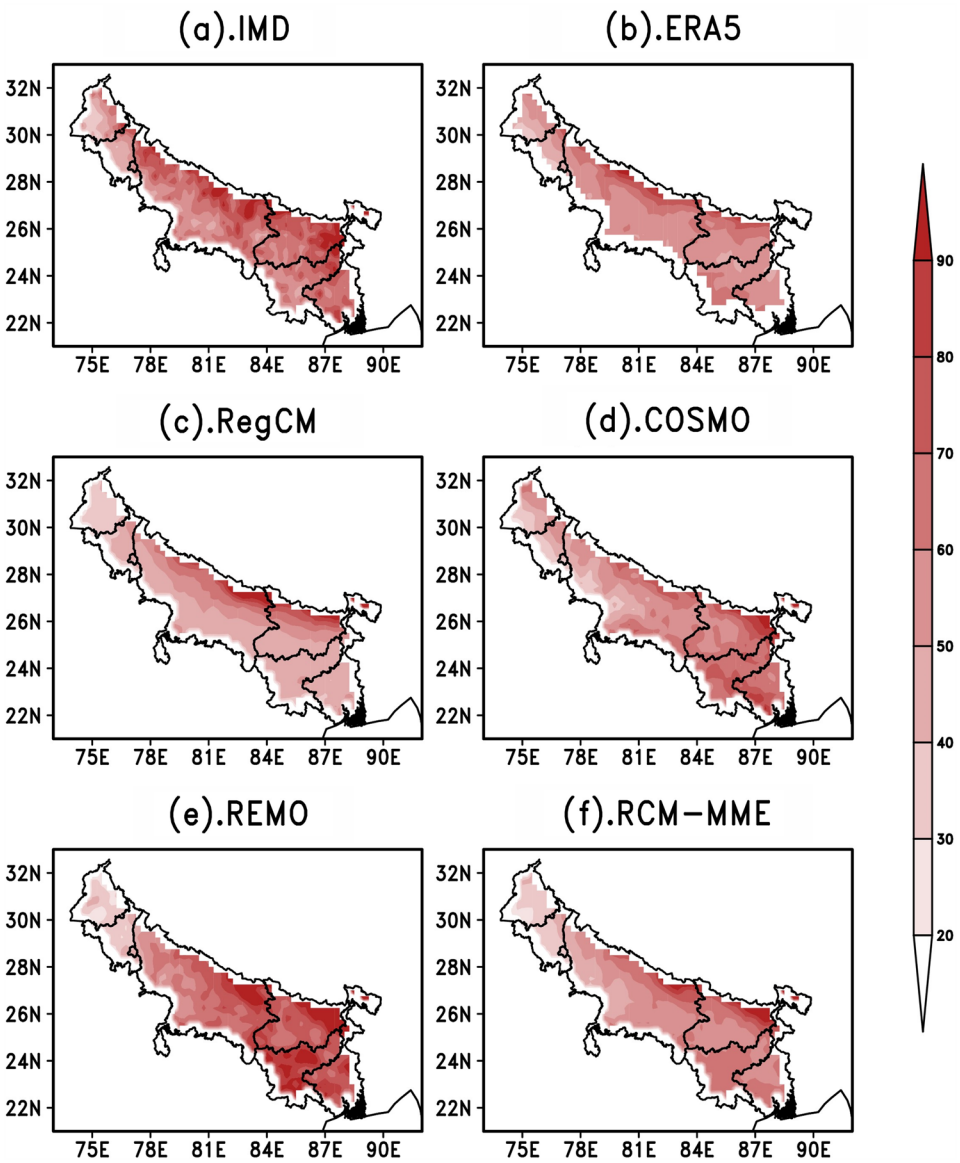

Fig. 6 Spatial distribution of observed and RCM simulated R95p thresholds (mm/day) during ISM season for the period 1981–2005 over IGP region

RCM-MME) have performed reasonably well in simulating the temperature at 850 hPa over the entire considered region (Fig. 9ib-e). However, COSMO has shown slight underestimations over IGP (Fig. 9di). Similarly, the distribution of MT depicts copious amounts of moisture being transported by strong low-level jet (more than 12 m/s) towards the Indian landmass (Fig. 9iia). The presence of plenty of moisture can be clearly seen over India and IGP regions in the ERA5 reanalysis pattern. Also, the availability of higher moisture content has been observed over the BoB region during extremely heavy rainfall days. A closure analysis reveals the availability of higher moisture content over the Western Ghats while lesser amount over the IGP region which might be the cause of lesser rainfall intensities during R95p days in ERA5 reanalysis (Fig. 6b). Further, a formation of cyclonic circulation possibly due to a low-pressure system over south-eastern lower IGP and adjoining regions of BoB can be noticed during the extreme rainfall events over IGP. The RCM simulations (including RCM-MME) also ensure that the distribution of MT along with wind is in good agreement with the ERA5 (Fig. 9iib-e). In RegCM the MT decreases near the sea-land boundary over the western coastal regions and hence central India which resembles the weakening of south-westerly winds in model simulation (Fig. 9iib). The REMO shows an underestimation of MT over the Somali coast and Western Ghats but it has robustly demonstrated the realistic patterns of the MT and wind pattern over BoB and Indian land including IGP (Fig. 9iic). Further, the member COSMO (Fig. 9iid) has performed exceptionally in simulating the MT and wind patterns over the entire considered region. However, it has shown excess/overestimations near western equatorial Indian Ocean

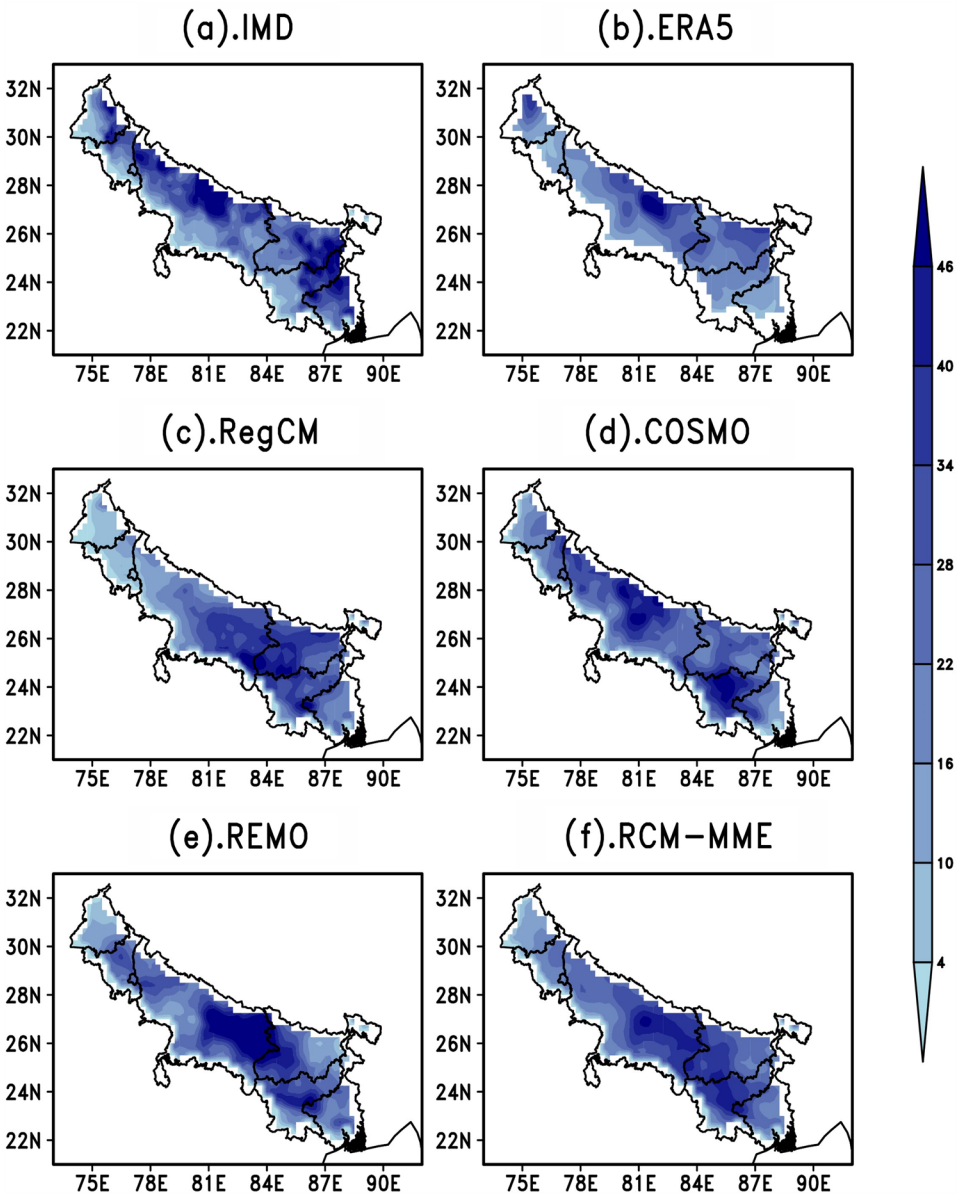

Fig. 7 Spatial distribution of observed and RCM simulated above mean rainfall (mm/day) on R95p days (composite) during ISM season for the period 1981–2005 over IGP region

regions during the R95p days. In order to analyse the moisture budget at a single level the HMFC has been computed at 850 hPa during the R95p days (Fig. 9iii). The reason behind considering a single level is the unavailability of considered RCM data sets in the public domain. However, a strong correlation at 850 hPa level between vertically integrated moisture transport (VIMFC) and HMFC has been reported in a study by Lee et al. 2017) which may be a good indicator to analyse the precipitation changes and associated extremes. The ERA5 reanalysis pattern shows higher convergence or positive HMFC (1–1.5KgKg^{-1} ms^{-1}) over the entire IGP, northeast and north-central Indian regions while divergence or negative HMFC -1.5 or more over western India and Western Ghat regions during the period (Fig. 9iiia). The intense convergence along the IGP and surrounding areas (including Himalayan foothills) considerably supports the occurrence of extremely heavy rainfall episodes. Also, moderate to higher convergence over the peninsular region along with divergence over its eastern coast region can be noticed. A moderate convergence (0.55KgKg^{-1} ms^{-1} or less) extending from the Somali coast to the Kerala coast and BoB region has been reported, contrary to that moderate to higher -0.5 to -15KgKg^{-1} ms^{-1} divergence over the northern Arabian sea has been observed during the R95p days. The RCM simulations have reproduced the observed HMFC pattern pretty well as compared with the ERA5 distribution (Fig. 9iiib–e). The RegCM highly underestimates the presence of convergence over IGP and adjoining regions which might be the cause behind the availability of lesser moisture and hence fewer rainfall

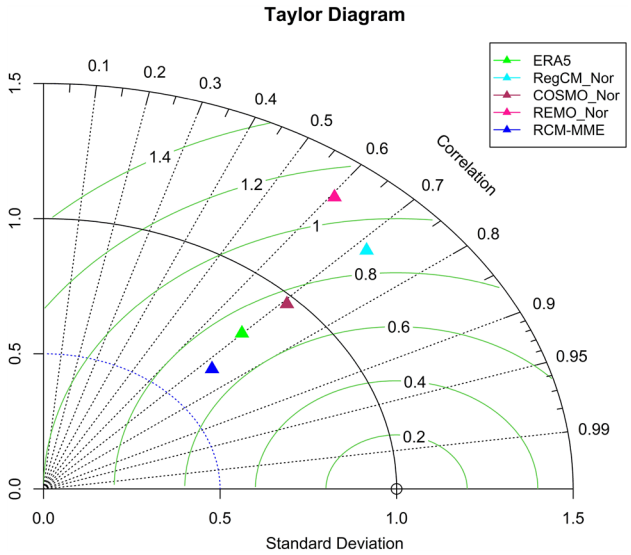

Fig. 8 Taylor's diagram for the RCM simulated mean R95p pattern (composite) during ISM season for the period 1981–2005 over the IGP region

Table 2 Total number of above R95p rainfall days during JJAS and monthly distribution of frequency of occurrence (in %)

Data sets	Total No. events (JJAS)	Distribution of events in each month (%)			
		June	July	August	September
IMD	25	8	20	32	40
ERA5	34	15	22	30	33
RegCM	22	25	10	20	45
COSMO	22	20	18	27	35
REMO	26	12	20	18	50
MME	28	17	15	23	45

intensities over the region during R95p days (Fig. 9iiib). Another member REMO performed satisfactorily in reproducing the presence of convergence over IGP and other concerned regions (Fig. 9iiic). However, it shows slight underestimations over central-north India. The COSMO performs robustly over entire considered regions including the oceanic regions (Fig. 9iiid). Among the discussed models so far, the COSMO produces the most realistic pattern of HMFC over the IGP region. The presence of divergence over the northern Arabian sea and convergence over the equatorial Indian Ocean is also well represented in COSMO simulations. The RCM-MME again results as an improvised approach for considered RCMs and produces more realistic patterns of HMFC over IGP and the entire domain during the period (Fig. 9iiie). To understand the occurrence of R95p days over IGP in depth further the anomalous composite patterns of geopotential height at 500 hPa (Zg500), vertical shear of zonal wind (VSZW;850 hPa-200 hPa), the moist static energy difference between levels 500 hPa and 925 hPa (MSE) and the water vapour path (PRW) has been computed (Fig. 10i–iv). Larger negative anomalies (− 12 to − 14 m) of Zg500 have been found to persist over the entire IGP and north India which resembles to the formation or presence of a low-pressure system (LPS) and can be used to denote the location of monsoon trough (Fig. 10ia). The smaller geopotential or more negative anomalies at the mid-troposphere along with more than 8 m/s winds at 850 hPa indicate the active monsoon activities over the region (Taniguchi and Koike 2006). Moderate negative anomalies (− 2 to − 4 m) have been reported over central India and western India while moderately high (4 to 6 m) Zg500 persists over peninsular regions. Further, the higher positive anomalies (8 m or more) can be seen over the eastern coast of peninsular India during the R95p days. The RCM simulations have shown the position of LPS over IGP and northern India with great accuracy (Fig. 10ib-d). However, the north-western stretch of LPS or lesser Zg500 is slightly underestimated in RegCM and REMO simulations. The northward spread of LPS is clearly visible in COSMO simulations which is much deeper than as reported in the ERA5 pattern but it has compromised the Zg500 over the lower IGP region (Fig. 10id). Further, the RCM-MME also represents the Zg500 pattern reasonably well during R95p days (Fig. 10ie). To support the present analysis dynamically, using conventional definitions, the vertical shear of zonal wind (VSZW) has been computed by considering the difference of lower level (u at 850 hPa) and upper level (u at 200 hPa) zonal wind (as defined by Mishra et al., (2022). The VSZW plays a crucial role in representing the northward shift of the convective band (Webster and Yang 1992; Mishra et al. 2022). The composite distribution pattern of VSZW anomalous pattern during R95p days has been illustrated in (Fig. 10ii). The ERA5 distribution shows maximum positive anomalies 5-6 m/s) over the entire IGP and adjoining regions while maximum negative anomalies (− 4 to − 5 m/s over the equatorial Indian Ocean and southern BoB regions which further extended towards peninsular India (Fig. 10iia). The Strengthening of zonal wind and VSZW prior to and during heavy rainfall activity over a region has been reported by Leena et al. 2022). Further, the Himalayan foothills also exhibit higher positive anomalies during the extreme rainfall over IGP. The RegCM fairly simulates the pattern but it has shown lesser positive anomalies over western India and central IGP regions (Fig. 10iib). Also, an overestimation of VSZW anomalies can be found over central and peninsular India in RegCM simulations. Another model REMO performs better than RegCM over almost the entire considered region (including IGP) except the equatorial Indian Ocean where it has shown an almost opposite pattern as that of ERA5 reanalysis (Fig. 10iic). The best-performing model so

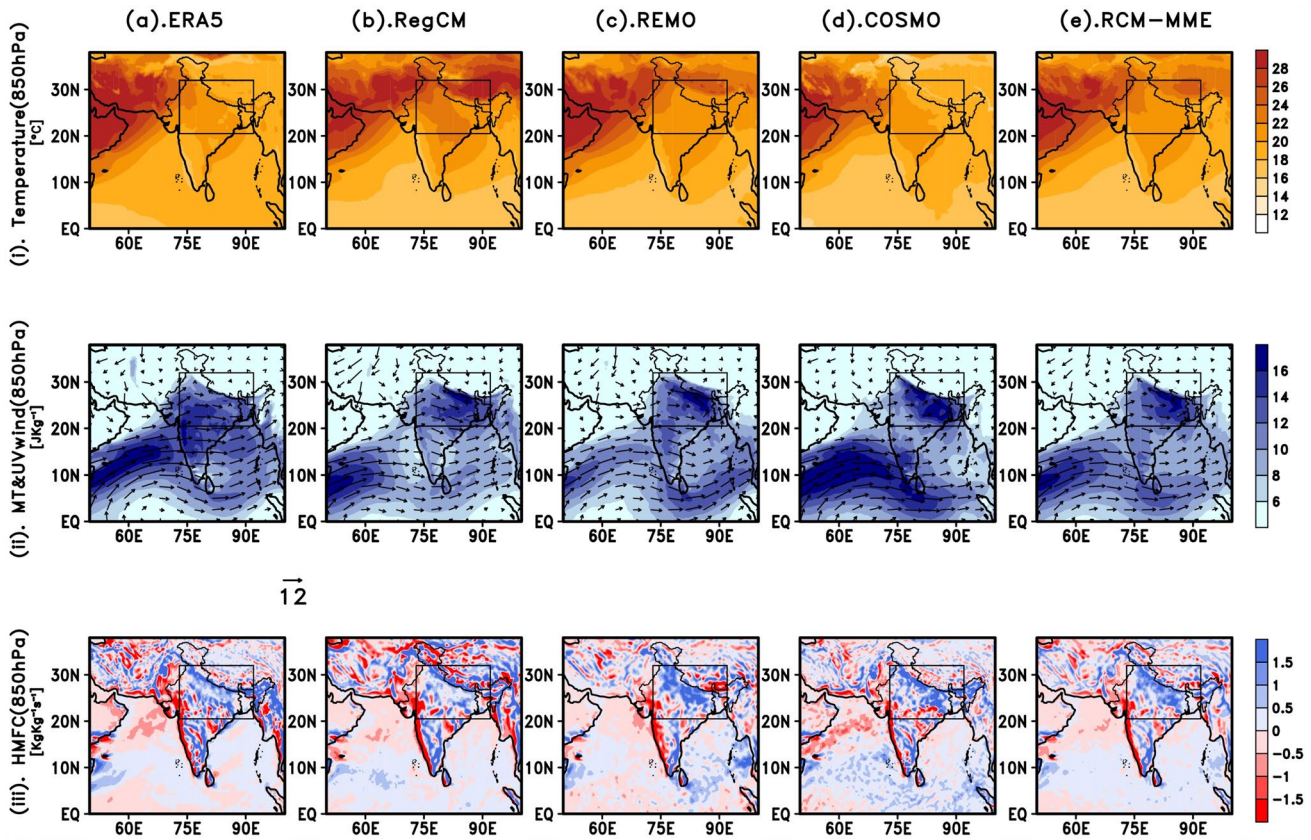

Fig. 9 Spatial distribution of reanalyses (ERA5) and RCM simulated mean (**i**). Temperature (T), (**ii**). MT & Wind and (**iii**). HMFC at 850 hPa on the days above R95p rainfall (composite) for ISM season during 1981–2005

far i.e., COSMO has robustly reproduced the VSZW pattern over the entire considered region with the least uncertainties over the domain (Fig. 10iid). Similarly, the RCM-MME also shows considerable patterns of VSZW during the R95p days (Fig. 10iie). The moist static energy (MSE) budget has been found to be a crucial factor in defining extended scale impacts of climate on convective rainfall and climatology of rainfall over tropical regions (Bretherton 2006;Maloney 2009; Schneider et al. 2014; Sobel et al. 2014). The atmospheric instability can be measured by the difference of moist static energy (MSE) near the surface and mid-tropospheric levels as it is analogous to the vertical gradient of the equivalent potential temperature over a region (Sooraj et al. 2020). The computed daily MSE (between 500 and 925 hPa levels) anomalous pattern of ERA5 reanalysis shows high MSE build-up (4000 J/Kg or more) over the entire IGP including Himalayan foothills during the R95p days over IGP (Fig. 10iiia). According to a study by Zheng et al., (2020) enhancement in column-integrated MSE represents the incursion of MSE from the surrounding which leads to the heating and moistening in an atmospheric column and induces deep convection. Further, some positive anomalies have also been reported in northeast India. Western India and most of the adjoining oceanic regions have shown light to higher negative anomalies during the rainfall extremes. The RegCM (Fig. 10iiib) underestimates MSE over upper and central IGP regions. However, it has reasonably performed elsewhere. The weaker MSE build-up and lesser VSZW in RegCM simulations can be a possible reason behind the dry biases and underestimation in extreme rainfall intensities over IGP. The COSMO has performed robustly over the entire considered region and the region of interest i.e., IGP closer to the ERA5 reanalysis pattern (Fig. 10iiid). However, it has shown some underestimations or opposite patterns over the heat-low region of ISM circulation. The REMO simulations also depict patterns closer to the ERA5 distribution over the entire IGP region with great accuracy. However, some overestimations can be noticed over the southern Indian region. Also, the RCM-MME have shown realistic MSE anomalous patterns over the considered region up to a great extent (Fig. 10iiie). At last, the distribution of water vapour path or total precipitable water (PRW) anomalies during the rainfall extremes over IGP have been illustrated in (Fig. 10iv). The occurrence of extremely heavy rainfall requires an enormous amount of precipitable water which can be quantified by the atmospheric water vapour

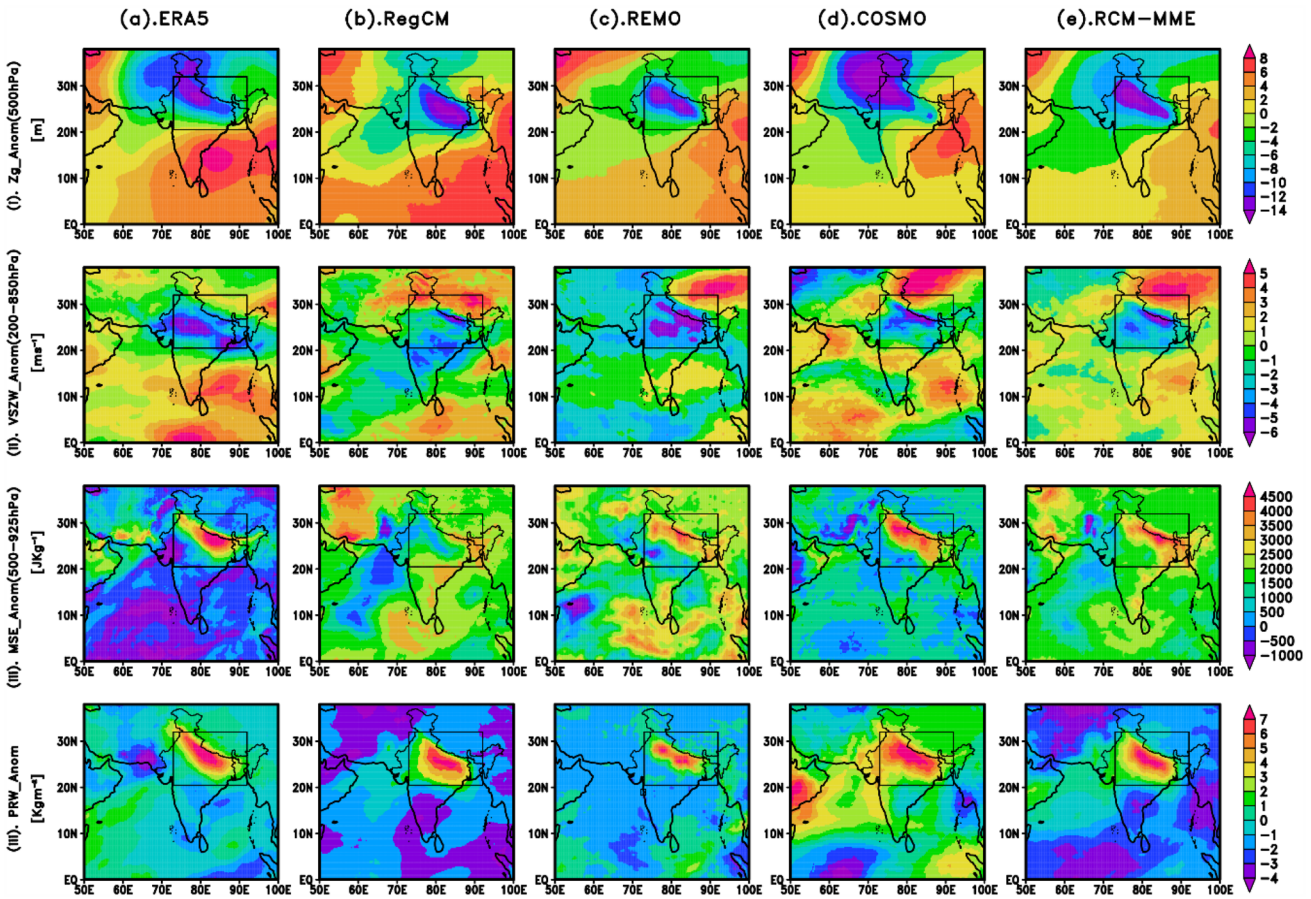

Fig. 10 Spatial distribution of reanalyses (ERA5) and RCM simulated anomalous patterns of (**i**). Zg500, (**ii**). VSZW, (**iii**). MSE difference between 500 and 850 hPa levels and (iv). PRW on the days above R95p rainfall (composite) for ISM season during 1981–2005

(Nayak et al. 2019). The presence of enormous precipitable water or maximum PRW anomalies (7 kg/m^2 or more) is clearly visible in ERA5 reanalysis distributions over IGP and adjoining regions during rainfall extremes (Fig. 10iva). The RegCM satisfactorily performs over almost the entire IGP in simulating the PRW patterns with great accuracy (Fig. 10ivb). However, it has shown underestimations over upper IGP regions. Similarly, the COSMO (Fig. 10ivd) also captures realistic PRW patterns over IGP but it has shown overestimations the PRW over the Western Ghats and northern Arabian sea. The RCM_MME technique again performs miraculously over the entire shown and IGP region of India during extremely heavy rainfall events (Fig. 10ive).

4.3.3 Evolution of rainfall extremes over IGP

In this section, the temporal evolution of synoptic patterns in the context of extreme rainfall events over IGP has been discussed. For that purpose, the RCM-MME composites of the previously discussed variables (Fig. 9&10) from 6 days prior (Lead6, Lead4, Lead2, Lead1) to the extreme/event day (Lag0) have been analysed (Figs. 11 and 12). The 850 hPa temperature shows the existence of negative anomalies (− 0.5 to − 0.8 °C) over IGP and some south Indian regions 6 days prior to the extreme rainfall events which subsequently decreases up to the extreme day (Fig. 11ia-e). On the other hand, positive anomalies (0.1 to 0.7 °C) or enhancement in temperature can be noticed over oceanic regions, especially over southern BoB and eastern Indian Ocean. Also, massive heating (0.7 to 1 °C or more) over the heat-low region can be seen 6 days prior to the extreme rainfall which extends towards the upper Arabian sea on the actual day of the event (Fig. 11ia–e). Similarly, the path of moisture transport by the LLJ and its strengthening (more than 10 m/s) is clearly visible (Fig. 11iia-e). The moisture-laden south-westerlies trace their path from the Somali coast to the Indian landmass and enormous amounts of moisture is transferred through the BoB branch of ISM circulation over IGP and adjoining regions from 6 days prior to the event day. The maximum moisture is present just before the day and on extreme rainfall days over the IGP region accompanied by a cyclonic circulation over eastern IGP (Fig. 11iid–e). The

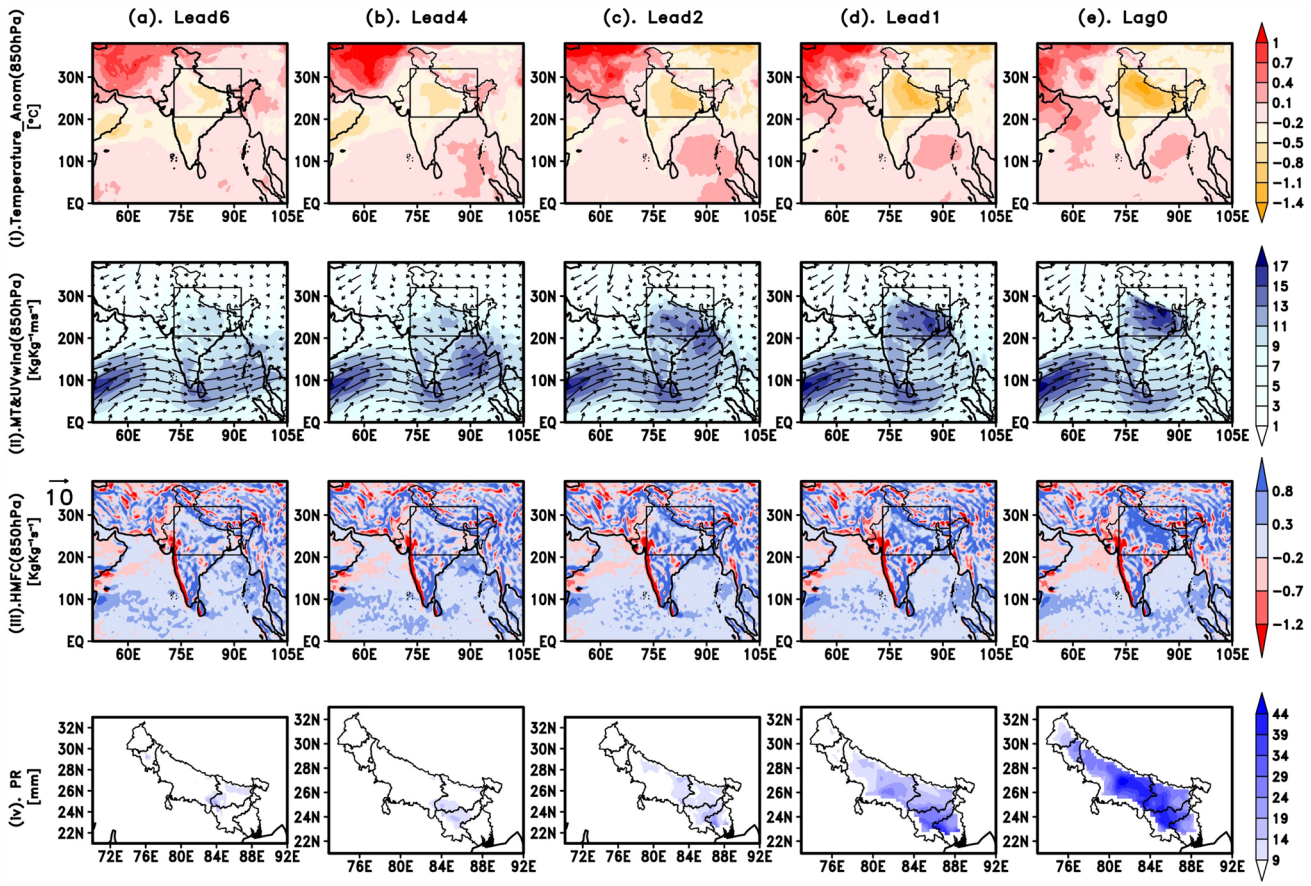

Fig. 11 Temporal evolution of RCM simulated (**i**). Temperature anomaly, (**ii**). MT & Wind, (**iii**). HMFC at 850 hPa and (**iv**). Rainfall (PR) on the R95p days (Composites) 6 days before (Lead6) to event day (Lag0) for ISM season during 1981–2005

HMFC pattern is also showing a build-up of slight to intense (0.2–0.3KgKg^{-1} ms^{-1} moisture convergence over IGP, central India and Himalayan foothills 6 days prior which substantially gets remarkably strong up to 2 days before the event day (Fig. 11iiia-c). The strongest HMFC can be clearly seen to be dominating over IGP and foothills just before and on the event day (Fig. 11iiid–e). A closure encounter reveals the presence of strong divergence over western India and Western Ghats 6 days prior to the event and remains present up to the R95p days (Fig. 11iiia–e). To understand the evolution of rainfall extremes over IGP in a better way the distribution of rainfall 6 days prior to the event days has been shown (Fig. 11iva–e). A moderate rainfall patch ~ 9 mm/day over lower IGP can be noticed over IGP 6 to 4 days prior (Fig. 11iva, b) which further increases towards central IGP with more intensity (24–29 mm/day) and at last maximum rainfall ranging from 29 to 44 mm/day or more over almost entire IGP is clearly visible on the event days which is in good agreement with the earlier discussed dynamical and thermodynamical aspects (Fig. 11ive). The above discussion suggests that Abrupt warming over the northern Arabian sea and southern BoB region triggers the enormous moisture transport with strong south-westerlies over the IGP region predominantly from the eastern coasts. Further, the cyclonic circulation over eastern IGP and adjoining coastal regions initiate higher convergence (higher HMFC) which further gets stronger and acquires almost the entire IGP on the event day. Along with moisture and wind convergence, it is also necessary to understand the evolution and growth of LPS or trough and instability measurements associated with rainfall extremes. The anomalous pattern of Zg500, VSZW, MSE and PRW has been depicted in (Fig. 12a–e). The presence of a LPS i.e., more negative Zg500 anomalies (− 15 to − 20 m) can be noticed over eastern BoB 6 days prior to the event day (Fig. 12ia). The trough gets deeper and spreads over a larger region from the Arabian sea to BoB with being deepest over the BoB region 4 days prior (Fig. 12ib) and subsequently moves north-westwards in upcoming days to get settled over IGP and adjoining regions on the day before the event day (Fig. 12ie). The presence of enormous moisture and strong LPS associated with higher convergence over IGP on or before the event day supports the occurrence of extreme rainfall over the region. As far as VSZW is concerned, positive anomalies are present over the entire region

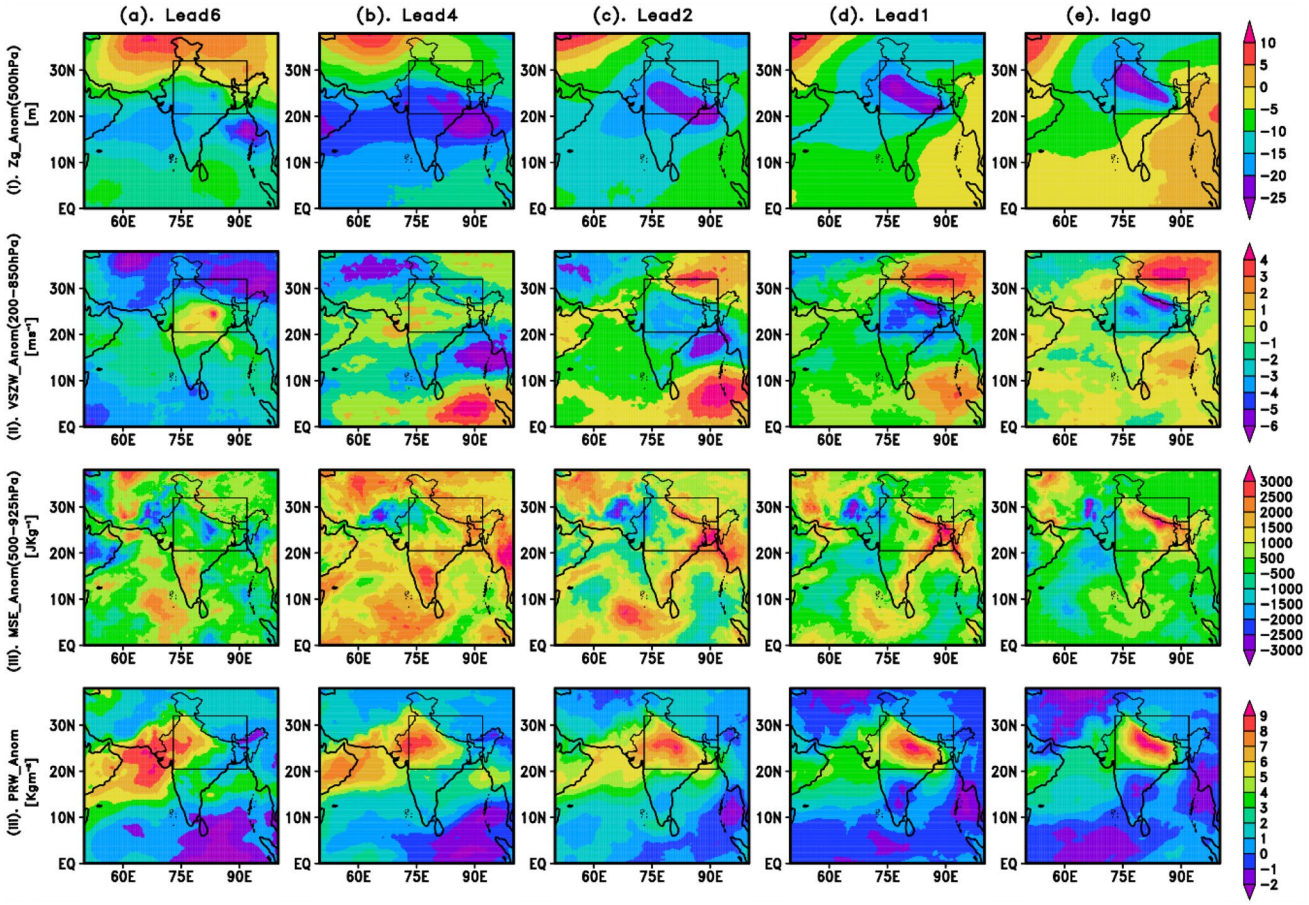

Fig. 12 Temporal evolution of RCM simulated anomalous patterns of (**i**). Zg500, (**ii**). VSZW, (**iii**). MSE and (**iv**). PRW on the R95p days (Composites) 6 days before (Lead6) to event day (Lag0) for ISM season during 1981–2005

except for some central India and IGP regions 6 days prior to event day which substantially gets enhanced in upcoming days (Fig. 12iia). An interesting pattern over BoB (higher positive anomalies up to 5 m/s) and the eastern Indian Ocean (negative anomaly up to − 4 m/s) 4 days prior to the event day has been noticed (Fig. 12iib). Further, the higher anomalous pattern shifts the north western ward and higher positive VSZW anomalies or strong VSZW gets developed over IGP 2 days prior to event day (Fig. 12iic). As the strong VSZW spreads over central India and IGP regions, the negative anomalous pattern over the eastern Indian Ocean starts becoming less negative and at the same time over the beyond Himalayas or Tibetan plateau region negative anomalies get prominent prior 2 and 1 day (Fig. 12iic–e). This shows a more or less northward propagating oscillatory pattern of VSZW near 90°E longitudes. To account for atmospheric instabilities the MSE anomalies (between the levels 500 hPa and 925 hPa) show higher build-up (1500–2500 J/Kg) over Indo-Pak arid region and west-south Ocean regions Lead6 and Lead4 days which extends towards peninsular India later on (Fig. 12iiia, b). Higher positive anomalous patterns (2500–3000 J/Kg or more) of MSE throughout the IGP and northeast India while lesser values elsewhere can be seen the day before and on the actual day of the extreme rainfall event (Fig. 12iiid, e). A closer encounter revealed negative anomalies (− 1500 to − 2500 J/Kg) over western India and heat-low regions on the event day (Fig. 12iiie). In a study Sooraj et al. (2020) found intense warming and higher MSE build-up over Indo-Pak arid regions as strong precursors of monsoon extremes over India. Finally, the evolution composite pattern of PRW anomalies has been illustrated in (Fig. 12iva–e). An enormous amount of precipitable water or higher positive anomalous pattern (8–9 kg/m^{-2}) has been reported over upper or northern Arabian sea regions which extend towards the Indian landmass 6 days prior to the event days (Fig. 12iva). Further, moving ahead in time this highly positive anomalous pattern of PRW gets shifted eastwards and ensures the presence of maximum PRW (anomalies being more than 9 kg/m^{-2}) over the entire IGP region day before and on the extreme event day (Fig. 12iib–e). All these underlying processes behind the occurrence of the extreme rainfall events over IGP in RCM-MME are consistence with

the ERA5 reanalysis data distributions (not shown here). To illustrate the previously discussed mechanism, a schematic diagram is presented in Fig. 13. The occurrence of extreme rainfall events in the IGP region is linked to the development of a LPS over the BoB at Lead6. Subsequently, this system advances towards the Indian landmass over time, settling over the IGP region prior and on the day of heavy rainfall (Lead1 and Lag0), resulting in advection of warm and moist air, facilitating enhanced moisture transport across the IGP region and the subsequent development of instabilities that supported the occurrence of heavy rainfall episodes.

5 Summary and conclusion

In the present study, a regional-specific- assessment of summer monsoon precipitation and associated extremes over one of the most fluvial fertile lands, the IGP has been performed for the period of 25 years (1981–2005). Analysis shows 1–10 mm/day of rainfall occurs over IGP in the summer monsoon season with the higher tail of the distribution lying over lower/eastern regions which subsequently decreases towards upper/western regions. The RCMs downscaled under the CORDEX-CORE framework have efficiently reproduced the mean summer precipitation patterns over the IGP region. The dynamical downscaling (at 25 km) using RCMs has robustly reduced the inherent biases present in parent data sets i.e., the Nor-ESM GCM. However, despite using a common initial and boundary conditions, inter-model differences in the considered RCM simulations stem. Which may be due to the variations in physical parameterizations for atmospheric processes like convection, radiation, cloud formation, and turbulence. Additionally, differences in model tuning, numerical methods, and time-stepping schemes impact simulation accuracy and stability, contributing to variations in the results.

Among all the considered RCMs, the performance of COSMO and RCM-MME is up to a great extent with the least biases across the region of interest. The statistical techniques used for validation also support the ability of RCMs in reducing the inherent uncertainties of parent GCM (Nor-ESM). To showcase the ISM dynamics, the distribution patterns of various parameters viz., temperature, moisture transport with wind, geopotential height and moist static energy

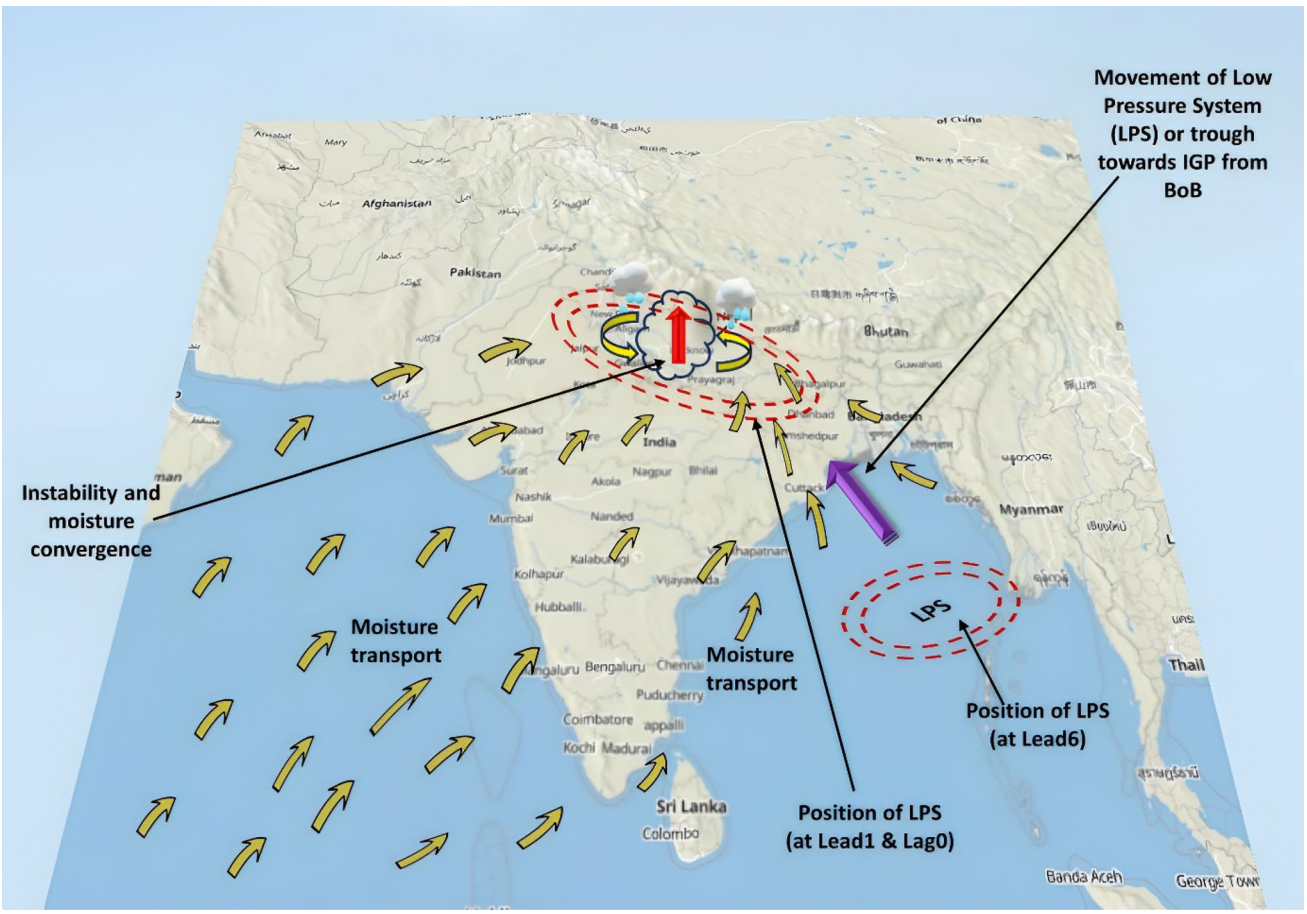

Fig. 13 A schematic diagram showing the mechanism behind the occurrence of heavy rainfall events over the IGP region during ISM season

at 850 hPa by considering ERA5 reanalysis as ground truth have been computed. The RCMs are able to simulate the ISM features such as the cross-equatorial flow, Somali jet, higher temperature over Indo-Pak arid region and presence of monsoon trough crossing Gangetic Plains. Further, the moist convection processes are supported by the intrusion of enormous moisture from the ocean to the Indian landmass and moist static energy build-up over central India and IGP regions which is clearly visible in RCM simulations. However, the patterns of COSMO and RCM-MME are much closer to ERA5 distribution than other models. Further, the persisting warm biases and moisture deficiency over the IGP region might be the cause of existing dry biases in RegCM and REMO simulations.

The identification of rainfall extremes over IGP has been done on the basis of above 95th percentile of daily rainfall occurring over the region of interest. Only the days covering a larger spatial extent (more than 20% of existing grids) have been considered. The 95th percentile thresholds lie on a wider range of 20–90 mm or more over different sectors of IGP. The upper tail of the distribution is concentrated over north-lower IGP and Himalayan foothills. Also, the composites of R95p days show 10-46 mm/day of rainfall over IGP which is well captured in RCM simulations, especially in COSMO. Further, a detailed comprehensive analysis to understand the underlying mechanism of rainfall extremes along with their evolution over IGP has been performed. For that purpose, in addition to earlier discussed parameters the composite patterns of HMFC, Zg500, VSZW, MSE and PRW have been considered. The ERA5 results indicate that the occurrence of extreme events in the IGP region is associated with a strong trough (i.e., a low-pressure system) located around the IGP region, leads to a strong advection of warm and moist air with enhanced moisture transport with the south-westerly flow from the Indian Ocean towards the IGP region resulting in precipitation due to convergence. The Zg500 clearly represents the presence of a deep trough which evolves at least 4 days prior over BoB and gets stretched and settles over the IGP region on the extreme rainfall day over IGP. A positive anomalous pattern of VSZW between 850 and 200 hPa also supports the genesis and occurrence of rainfall extremes over IGP during the considered period which is clearly visible in RCM simulations. The thermodynamic response is strongly supported by the intense HMFC at 850 hPa and higher MSE build-up between levels 500 and 925 hPa which causes atmospheric instabilities at the regional level. This thermodynamics support is not up to the mark in RegCM simulations which might be the region behind comparatively poorer performance in reproducing rainfall extremes over IGP. However, the model COSMO efficiently demonstrates favourable conditions for heavy rainfall in both dynamical and thermodynamical aspects. The COSMO has been employed in non-hydrostatic mode, according to Holton (2004), the non-hydrostatic core provides a better representation of the convective phenomena particularly for the heavy rainfall cases. Due to their efficient performance, non-hydrostatic models are suitable for short to medium-range forecasts of atmospheric phenomenon such as cyclones, monsoon depression and heavy rainfall (Dudhia 1993; Mukhopadhyay and Nanjundiah 2018). However, both the RCMs (COSMO and RegCM) satisfactorily estimated the amount of PRW during and prior to the events. This study provides a first-ever detailed mechanism analysis of rainfall extremes over a socioeconomically vulnerable region of the country. The efficiency of high-resolution CORDEX-CORE simulations in representing the rainfall extremes and underlying mechanisms at localized scales with their evolution 6 days prior as precursors is robustly demonstrated. This study might be useful for various researchers and the climate modelling community in analyzing and predicting rainfall extremes at regional scales. Also, this may provide a way forward for climatologists and policymakers to develop and implement reasonable mitigation strategies in order to face the challenges of climate change in a warming climate.

Acknowledgements The present study forms a component of MP's doctoral dissertation and has received support from a R&D project funded by the DST, Govt. of India. The authors wish to extend their appreciation to the two anonymous reviewers for their valuable suggestions, which greatly improved the quality of this manuscript. RB also acknowledges the IOE grant under Dev. Scheme 6031(A). The authors would like to express their gratitude to the WCRP community for initiating the CORDEX project. Authors are also thankful to the IMD, ECMWF and GERICS for providing the data utilized in this study.

Author contributions This paper is conceptualized by MP, NKS and RB which is further designed by MP and NKS. Authors MP, NKS and RB further developed the research plan. AR provided the REMO simulated data sets. MP and NKS did the data processing and the analyses under the guidance of RB and AR. MP wrote the first draft, which was subsequently modified by NKS and AR. RB, RKM and SS supervised the research work. The manuscript has been thoroughly reviewed by all the authors, who have contributed their expertise to enhance the quality of the work and have given their approval by accepting the authors' agreement.

Funding Not applicable.

Data availability statement The datasets generated during and/or analysed during the current study are available from the corresponding author upon reasonable request.

Declarations

Conflict of interest The authors declare that they have no known competing financial interests or personal relationships that could have appeared to influence the work reported in this paper.

References

Allen MR, Ingram WJ (2002) Constraints on future changes in climate and the hydrologic cycle. Nature 419(6903):224–232

Asharaf S, Ahrens B (2015) Indian summer monsoon rainfall processes in climate change scenarios. J Clim 28(13):5414–5429
Ashfaq M, Cavazos T, Reboita MS, Torres-Alavez JA, Im E-S, Olusegun CF, Alves L, Key K, Adeniyi MO, Tall M (2021) Robust late twenty-first century shift in the regional monsoons in RegCM-CORDEX simulations. Clim Dyn 57:1463–1488
Bajrang C, Attada R, Goswami BN (2023) Possible factors for the recent changes in frequency of central Indian Summer Monsoon precipitation extremes during 2005–2020. Npj Clim Atmos Sci 6(1):120
Baldauf M, Seifert A, Förstner J, Majewski D, Raschendorfer M, Reinhardt T (2011) Operational convective-scale numerical weather prediction with the COSMO model: description and sensitivities. Mon Weather Rev 139(12):3887–3905
Bentsen M, Bethke I, Debernard JB, Iversen T, Kirkevåg A, Seland Ø, Drange H, Roelandt C, Seierstad IA, Hoose C (2013) The Norwegian Earth System Model, NorESM1-M–Part 1: description and basic evaluation of the physical climate. Geosci Model Dev 6:687–720
Bhatla R, Singh M, Mall R, Tripathi A, Raju P (2015) Variability of summer monsoon rainfall over Indo-Gangetic Plains in relation to El-Nino/La-Nina. Nat Hazards 78:837–853
Bhatla R, Ghosh S, Mandal B, Mall R, Sharma K (2016) Simulation of Indian summer monsoon onset with different parameterization convection schemes of RegCM-4.3. Atmos Res 176:10–18
Bhatla R, Ghosh S, Mall R, Sinha P, Sarkar A (2018) Regional climate model performance in simulating intra-seasonal and interannual variability of Indian summer monsoon. Pure Appl Geophys 175(10):3697–3718
Bhatla R, Verma S, Ghosh S, Mall RK (2019a) Performance of regional climate model in simulating Indian summer monsoon over Indian homogeneous region. Theor Appl Clim 176:1–15
Bhatla R, Verma S, Pandey R et al (2019b) Evolution of extreme rainfall events over indo-gangetic plain in changing climate during 1901–2010. J Earth Syst Sci 128:1–14
Bhatla R, Varma P, Verma S, Ghosh S (2020) El Nino/La Nina impact on crop production over different agroclimatic zones of Indo-Gangetic Plain of India. Theor Appl Climatol 142:151–163
Bollasina M, Nigam S (2011) The summertime "heat" low over Pakistan/northwestern India: evolution and origin. Clim Dyn 37:957–970
Bretherton CS (2006) Moisture transport, lower-tropospheric stability, and decoupling of cloud-topped boundary layers. J Atmos Sci 63(9):2436–2451
Chaturvedi RK, Joshi J, Jayaraman M, Bala G, Ravindranath NH (2012) Multi-model climate change projections for India under representative concentration pathways. Curr Sci 103(8):791–802
Chauhan BS, Mahajan G, Randhawa RK, Singh H, Kang MS (2014) Global warming and its possible impact on agriculture in India. Adv Agron 123:65–121
Choudhary A, Dimri AP (2018) Assessment of CORDEX-South Asia experiments for monsoonal precipitation over Himalayan region for future climate. Clim Dyn 50:3009–3030
Choudhary A, Dimri AP (2019) On bias correction of summer monsoon precipitation over India from CORDEX-SA simulations. Int J Climatol 39(3):1388–1403
Choudhury G, Tyagi B, Vissa NK, Singh J, Sarangi C, Tripathi SN, Tesche M (2020) Aerosol-enhanced high precipitation events near the Himalayan foothills. Atmos Chem Phys 20(23):15389–15399
Dudhia J (1993) A nonhydrostatic version of the Penn State-NCAR mesoscale model: validation tests. Mon Weather Rev 121:1493–1513
Endo H, Kitoh A (2014) Thermodynamic and dynamic effects on regional monsoon rainfall changes in a warmer climate. Geophys Res Lett 41(5):1704–1711
Fadhel S, Rico-Ramirez MA, Han D (2018) Sensitivity of peak flow to the change of rainfall temporal pattern due to warmer climate. J Hydrol 560:546–559
Fan J, Rosenfeld D, Yang Y, Zhao C, Leung LR, Li Z (2015) Substantial contribution of anthropogenic air pollution to catastrophic floods in Southwest China. Geophys Res Lett 42(14):6066–6075
Field CB, Barros V, Stocker TF, Dahe Q (eds) (2012) Managing the risks of extreme events and disasters to advance climate change adaptation: special report of the intergovernmental panel on climate change. Cambridge University Press, Cambridge
Freychet N, Hsu HH, Chou C, Wu CH (2015) Asian summer monsoon in CMIP5 projections: A link between the change in extreme precipitation and monsoon dynamics. J Clim 28(4):1477–1493
Gadgil S (2003) The Indian monsoon and its variability. Annual Rev Earth Planet Sci 31:429–467. https://doi.org/10.1146/annurev.earth.31.100901.141251
Gadgil S, Rupa Kumar K (2006) The Asian monsoon—agriculture and economy. The Asian Monsoon, Springer, Berlin Heidelberg, Cham, pp 651–683
Ghosh S, Bhatla R, Mall R, Srivastava PK, Sahai A (2019) Aspect of ECMWF downscaled Regional Climate Modeling in simulating Indian summer monsoon rainfall and dependencies on lateral boundary conditions. Theor Appl Climatol 135:1559–1581
Ghosh S, Sinha P, Bhatla R, Mall RK, Sarkar A (2022) Assessment of Lead-Lag and Spatial Changes in simulating different epochs of the Indian summer monsoon using RegCM4. Atmos Res 265:105892. https://doi.org/10.1016/j.atmosres.2021.105892
Ghosh S, Sarkar A, Bhatla R, Mall RK, Payra S, Gupta P (2023) Changes in the mechanism of the South-Asian summer monsoon onset propagation induced by the pre-monsoon aerosol dust storm. Atmos Res 294:106980
Giorgi F, Gutowski WJ Jr (2015) Regional dynamical downscaling and the CORDEX initiative. Annu Rev Environ Resour 40:467–490
Giorgi F, Jones C, Asrar GR (2009) Addressing climate information needs at the regional level: The CORDEX framework. World Meteorol Org Bull 58(3):175–183
Giorgi F, Coppola E, Solmon F, Mariotti L, Sylla MB, Bi X, Brankovic C (2012) RegCM4: model description and preliminary tests over multiple CORDEX domains. Clim Res 52:7–29
Giorgi F, Coppola E, Teichmann C, Jacob D (2021) Editorial for the CORDEX-CORE experiment I special issue. Clim Dyn 57(5–6):1265–1268
Goswami BN, Venugopal V, Sengupta D, Madhusoodanan M, Xavier PK (2006) Increasing trend of extreme rain events over India in a warming environment. Science 314(5804):1442–1445
Goswami, B. N. (2005) South Asian monsoon: intraseasonal variability. In The Asian monsoon (pp. 125–166) Springer, Berlin, Heidelberg.
Groisman PY, Knight RW, Karl TR, Easterling DR, Sun B, Lawrimore JH (2005) Contemporary changes of the hydrological cycle over the contiguous United States: trends derived from in situ observations. J Hydrometeorol 5:64–85
Gusain A, Ghosh S, Karmakar S (2020) Added value of CMIP6 over CMIP5 models in simulating Indian summer monsoon rainfall. Atmos Res 232:104680
Hersbach H, Bell B, Berrisford P, Hirahara S, Horányi A, Muñoz-Sabater J, Thépaut JN (2020) The ERA5 global reanalysis. Quart J R Meteorol Soc 146(730):1999–2049
Holton JR (2004) An Introduction to Dynamic Meteorology, Academic Press, International Geophysics Series Volume 88, Fourth Edition, 535 p., ISBN 0–12–354015–1, ISBN 978–0–12–354015–7
Intergovernmental Panel on Climate Change (IPCC) (2013) In: Stocker TF et al (Eds) Climate change (2013): the physical science basis. Contribution of working group I to the fifth

assessment report of the Intergovernmental Panel on Climate Change. Cambridge University Press, Cambridge

Jacob D, Elizalde A, Haensler A, Hagemann S, Kumar P, Podzun R, Wilhelm C (2012) Assessing the transferability of the regional climate model REMO to different coordinated regional climate downscaling experiment (CORDEX) regions. Atmosphere 3(1):181–199

Joseph S, Sahai A, Sharmila S, Abhilash S, Borah N, Chattopadhyay R, Pillai P, Rajeevan M, Kumar A (2015) North Indian heavy rainfall event during June 2013: diagnostics and extended range prediction. Clim Dyn 44:2049–2065

Gutowski JrJ, Giorgi F, Timbal B, Frigon A, Jacob D, Kang, HS, Santer, B (2016) WCRP CORDEX: Science and regional climate downscaling. In Climate Vulnerability (pp. 29–50) Academic Press

Kale VS (2003) Geomorphic effects of monsoon floods on Indian rivers. Nat Hazards 28:65–84

Kang IS, Yang YM, Tao WK (2015) GCMs with implicit and explicit representation of cloud microphysics for simulation of extreme precipitation frequency. Clim Dyn 45(1–2):325–335

Kumar P, Wiltshire A, Mathison C, Asharaf S, Ahrens B, Lucas-Picher et al. (2013) Downscaled climate change projections with uncertainty assessment over India using a high resolution multi-model approach. Sci Total Environ 468:S18–S30

Lee D, Min SK, Jin J, Lee JW, Cha DH, Suh MS, Joh M (2017) Thermodynamic and dynamic contributions to future changes in summer precipitation over Northeast Asia and Korea: a multi-RCM study. Clim Dyn 49:4121–4139

Leena PP, Sanket BR, Kumar VA et al (2022) Observed features of monsoon low-level jet and its relationship with rainfall activity over a high-altitude site in Western Ghats, India. Theor Appl Climatol 150:551–565

Maharana P, Dimri AP (2014) Simulation of the Indian summer monsoon precipitation using RegCM4: Sensitivity to convective schemes. Theoret Appl Climatol 118(1–2):277–295

Maharana P, Dimri AP (2016) Simulating Indian summer monsoon with RegCM4: model configuration and resolution study. J Earth Syst Sci 125(2):249–266

Maharana P, Pattnaik S, Ramesh KJ (2019) Improved Indian summer monsoon simulation by RegCM4 6 for the present climate. Int J Climatol 39(2):811–828. https://doi.org/10.1002/joc.5847

Maharana P, Kumar D, Das S, Tiwari PR (2021) Present and future changes in precipitation characteristics during Indian summer monsoon in CORDEX-CORE simulations. Int J Climatol 41(3):2137– 2153

Maity R, Aggarwal A, Chanda K (2016) Do CMIP5 models hint at a warmer and wetter India in the 21st century? J Water Clim Change 7(2):280–295

Maloney ED (2009) The moist static energy budget of a composite tropical intraseasonal oscillation in a climate model. J Clim 22(3):711–729

Mishra V, Shah HL (2018) Hydroclimatological perspective of the Kerala flood of 2018. J Geol Soc India 92(5):645–650

Mishra AK, Kumar P, Dubey AK, Tiwari G, Sein DV (2022) Impact of air–sea coupling on the simulation of Indian summer monsoon using a high-resolution Regional Earth System Model over CORDEX-SA. Clim Dyn 59(9–10):3013–3033

Mukhopadhyay P, Nanjundiah RS (2018) Representation of physical processes in weather and climate models. Curr Sci 114:1155

Nayak S, Takemi T (2019) Dependence of extreme precipitable water events on temperature. Atmósfera 32(2):159–165

New M, Rahiz M, Karmacharya J (2012) Climate change in Indo-Gangetic agriculture: Recent trends, current projections, crop-climate suitability, and prospects for improved climate model information. CGIAR Research Program on Climate Change, Agriculture and Food Security (CCAFS), Copenhagen, Denmark, 3–18

Nikumbh AC, Chakraborty A, Bhat GS (2019) Recent spatial aggregation tendency of rainfall extremes over India. Sci Rep 9(1):10321

Pai D, Rajeevan M, Sreejith O, Mukhopadhyay B, Satbha N (2014) Development of a new high spatial resolution (0.25× 0.25) long period (1901–2010) daily gridded rainfall data set over India and its comparison with existing data sets over the region. Mausam 65(1):1–18

Pal JS, Giorgi F, Bi X, Elguindi N, Solmon F, Gao X, Ashfaq M (2007) Regional climate modeling for the developing world: the ICTP RegCM3 and RegCNET. Bull Am Meteorol Soc 88(9):1395–1410

Pal D, Bhattacharyya T, Srivastava P, Chandran P, Ray S (2009) Soils of the Indo-Gangetic Plains: their historical perspective and management. Curr Sci 96:1193–1202

Pant M, Ghosh S, Verma S, Sinha P, Mall RK, Bhatla R (2022) Simulation of an extreme rainfall event over Mumbai using a regional climate model a case study. Meteorol Atmos Phys. https://doi.org/10.1007/s00703-021-00845-7

Pant M, Bhatla R, Ghosh S et al (2023a) Will warming climate affect the characteristics of summer monsoon rainfall and associated extremes over the Gangetic Plains in India? Earth Space Sci 10(2):e2022EA002741

Pant M, Bhatla R, Ghosh S, Das S, Mall RK (2023b) How climate change is affecting the summer monsoon extreme rainfall pattern over the Indo-Gangetic Plains of India: present and future perspectives. Clim Dyn 62:1–21

Prakash S, Mitra AK, Momin IM, Pai DS, Rajagopal EN, Basu S (2015) Comparison of TMPA-3B42 versions 6 and 7 precipitation products with gauge-based data over India for the southwest monsoon period. J Hydrometeorol 16(1):346–362

Rajeevan M, Bhate J, Jaswal AK (2008) Analysis of variability and trends of extreme rainfall events over India using 104 years of gridded daily rainfall data. Geophys Res Lett. https://doi.org/10.1029/2008GL035143

Ramesh KV, Goswami P (2014) Assessing reliability of regional climate projections: the case of Indian monsoon. Sci Rep 4(1):4071

Rana A, Nikulin G, Kjellström E, Strandberg G, Kupiainen M, Hansson U, Kolax M (2020) Contrasting regional and global climate simulations over South Asia. Clim Dyn 54:2883–2901

Rani SI, Arulalan T, George JP, Rajagopal EN, Renshaw R, Maycock A, Barker DM, Rajeevan M (2021) IMDAA: High-resolution satellite-era reanalysis for the Indian monsoon region. J Clim 34:5109–5133

Remedio AR, Teichmann C, Buntemeyer L, Sieck K, Weber T, Rechid D, Jacob D (2019) Evaluation of new CORDEX simulations using an updated Köppen-Trewartha climate classification. Atmosphere 10(11):726

Rogelj J, Forster PM, Kriegler E, Smith CJ, Séférian R (2019) Estimating and tracking the remaining carbon budget for stringent climate targets. Nature 571:335–342

Roxy MK, Ghosh S, Pathak A, Athulya R, Mujumdar M, Murtugudde R, Rajeevan M (2017) A threefold rise in widespread extreme rain events over central India. Nat Commun 8(1):1–11

Saha U, Sateesh M (2022) Rainfall extremes on the rise: Observations during 1951–2020 and bias-corrected CMIP6 projections for near-and late 21st century over Indian landmass. J Hydrol 608:127682

Sanjay J, Krishnan R, Shrestha AB, Rajbhandari R, Ren GY (2017) Downscaled climate change projections for the Hindu Kush Himalayan region using CORDEX South Asia regional climate models. Adv Clim Chang Res 8(3):185–198

Sanjay J, Ramarao MVS, Mahesh R, Ingle S, Singh BB, & Krishnan R (2020) Regional climate change datasets for South Asia. arXiv preprint arXiv:2012.10387.
Schneider T, Bischoff T, Haug GH (2014) Migrations and dynamics of the intertropical convergence zone. Nature 513(7516):45–53
Shahi NK, Rai S (2023) An increase in widespread extreme precipitation events during the northeast monsoon season over south peninsular India. Sci Rep 13:22757. https://doi.org/10.1038/s41598-023-50324-9
Shahi NK, Rai S, Mishra N (2018) Southern Indian Ocean SST as a modulator for the progression of Indian summer monsoon. Theor Appl Climatol 131:705–717
Shahi NK, Das S, Ghosh S, Maharana P, Rai S (2021) Projected changes in the mean and intra-seasonal variability of the Indian summer monsoon in the RegCM CORDEX-CORE simulations under higher warming conditions. Clim Dyn 57:1489–1506
Shahi NK, Polcher J, Bastin S, Pennel R, Fita L (2022) Assessment of the spatio-temporal variability of the added value on precipitation of convection-permitting simulation over the Iberian Peninsula using the RegIPSL regional earth system model. Clim Dyn 59(1–2):471–498
Sharmila S, Pillai PA, Joseph S, Roxy M, Krishna RPM, Chattopadhyay R, Goswami BN (2013) Role of ocean–atmosphere interaction on northward propagation of Indian summer monsoon intra-seasonal oscillations (MISO). Clim Dyn 41:1651–1669
Sharmila S, Joseph S, Sahai A, Abhilash S, Chattopadhyay R (2015) Future projection of Indian summer monsoon variability under climate change scenario: an assessment from CMIP5 climate models. Global Planet Change 124:62–78
Singh M, Bhatla R (2020) Intense rainfall conditions over Indo-Gangetic Plains under the influence of Madden–Julian Oscillation. Meteorol Atmos Phys 132:441–449
Singh V, Goyal MK (2016) Analysis and trends of precipitation lapse rate and extreme indices over north Sikkim eastern Himalayas under CMIP5ESM-2M RCPs experiments. Atmos Res 167:34–60
Singh N, Sontakke N (2002) On climatic fluctuations and environmental changes of the Indo-Gangetic Plains, India. Clim Chang 52:287–313
Singh S, Ghosh S, Sahana A, Vittal H, Karmakar S (2017) Do dynamic regional models add value to the global model projections of Indian monsoon? Clim Dyn 48(3):1375–1397
Sinha P, Mohanty UC, Kar SC, Dash SK, Kumari S (2013) Sensitivity of the GCM driven summer monsoon simulations to cumulus parameterization schemes in nested RegCM3. Theor Appl Climatol 112:285–306
Sobel A, Wang S, Kim D (2014) Moist static energy budget of the MJO during DYNAMO. J Atmos Sci 71(11):4276–4291
Sooraj KP, Terray P, Shilin A, Mujumdar M (2020) Dynamics of rainfall extremes over India: a new perspective. Int J Climatol 40(12):5223–5245
Sørland SL, Brogli R, Pothapakula PK, Russo E, Van de Walle J, Ahrens B, Thiery W (2021) COSMO-CLM regional climate simulations in the Coordinated Regional Climate Downscaling Experiment (CORDEX) framework: a review. Geosci Model Dev 14(8):5125–5154
Taniguchi K, Koike T (2006) Comparison of definitions of Indian summer monsoon onset: better representation of rapid transitions of atmospheric conditions. Geophys Res Lett. https://doi.org/10.1029/2005GL024526
Taylor KE (2001) Summarizing multiple aspects of model performance in a single diagram. J Geophys Res 106(D7):7183–7192
Teichmann C, Jacob D, Remedio AR et al (2021) Assessing mean climate change signals in the global CORDEX-CORE ensemble. Clim Dyn 57:1269–1292. https://doi.org/10.1007/s00382-020-05494-x
Thompson DW, Wallace JM (1998) The Arctic Oscillation signature in the wintertime geopotential height and temperature fields. Geophys Res Lett 25(9):1297–1300
Trenberth KE, Dai A, Rasmussen RM, Parsons DB (2003) The changing character of precipitation. Bull Am Meteor Soc 84(9):1205–1218
Varikoden H, Mujumdar M, Revadekar JV, Sooraj KP, Ramarao MVS, Sanjay J, Krishnan R (2018) Assessment of regional downscaling simulations for long term mean, excess and deficit Indian Summer Monsoons. Global Planet Change 162:28–38
Verma S, Bhatla R, Ghosh S, Sinha P, Kumar Mall R, Pant M (2021) Spatio-temporal variability of summer monsoon surface air temperature over India and its regions using Regional Climate Model. Int J Climatol 41:5820–5842
Verma A, Rakhecha PR, Yadav RK (2022a) Improved simulation of Indian Summer Monsoon Rainfall with the CORDEX South Asia Regional Climate Models. Pure Appl Geophys 179(2):613–632. https://doi.org/10.1007/s00024-021-02733-x
Verma S, Bhatla R, Shahi NK, Mall RK (2022b) Regional modulating behavior of Indian summer monsoon rainfall in context of spatio-temporal variation of drought and flood events. Atmos Res 274:106201
Verma S, Bhatla R, Singh PK (2023) Understanding the association of tropical SST anomalies on the ISMR during extreme IOD events. Pure Appl Geophys. https://doi.org/10.1007/s00024-023-03394-9
Vittal H et al (2016) Lack of dependence of indian summer monsoon rainfall extremes. Sci Rep. https://doi.org/10.1038/srep31039
Wang C, Kim D, Ekman AM, Barth MC, Rasch PJ (2009) Impact of anthropogenic aerosols on Indian summer monsoon. Geophys Res Lett. https://doi.org/10.1029/2009GL040114
Wang B (2006) The Asian Monsoon. Springer Science & Business Media
Webster PJ, Yang S (1992) Monsoon and ENSO: Selectively interactive systems. Q J R Meteorol Soc 118(507):877–926
Woo S, Singh GP, Oh JH, Lee KM (2019) Projection of seasonal summer precipitation over Indian sub-continent with a high-resolution AGCM based on the RCP scenarios. Meteorol Atmos Phys 131:897–916
Xu Y, Ramanathan V, Victor DG (2018) Global warming will happen faster than we think. Nature 564:30–32
Yaduvanshi A, Ranade A (2017) Long-term rainfall variability in the eastern gangetic plain in relation to global temperature change. Atmos Ocean 55(2):94–109
Yu L, Wu S, Ma Z (2019) Evaluation of moist static energy in a simulated tropical cyclone. Atmosphere 10(6):319
Zheng T, Feng T, Xu K, Cheng X (2020) Precipitation and the associated moist static energy budget off western Australia in conjunction with Ningaloo Niño. Front Earth Sci 8:597915